

## Thrust tectonics in the North Patagonian Massif (Argentina): Implications for a Patagonia plate

W. von Gosen

Geological Institute, University of Erlangen-Nürnberg, Erlangen, Germany

Received 4 September 2001; revised 28 February 2002; accepted 4 June 2002; published 21 February 2003.

[1] In the northeastern segment of the North Patagonian Massif (southern Argentina), S to SW directed thrusting affected a Late Proterozoic to Cambrian phyllite succession and the Silurian to Lower Devonian Sierra Grande formation. Thrust tectonics was partly combined with the formation of mylonites and followed by the intrusion of the Navarrete granodiorite. Mylonites of the Tardugno granitoids are attributed to a ductile shear horizon in the subsurface. As second stage of deformation after cessation of thrusting, ~NW-SE compression led to the formation of widely distributed fold structures around NE-SW trending axes as well as SE directed reverse faults. It was followed by the late kinematic intrusion of a porphyric granite as final pulse of the Navarrete Intrusive Complex. Local folding around ~N-S to NW-SE trending axes represents the final stage of the compressive deformational history. Thrust tectonics plus subsequent stages of deformation can be assigned to the Late Paleozoic time interval, probably the Permian. They are seen in conjunction with the formation of granite mylonites within the North Patagonian Massif, the Cerro de los Viejos granite mylonite of the La Pampa Province, and the compressive structures in the Sierras Australes fold-and-thrust belt north of the boundary between Patagonia and Gondwana South America. Also, the lack of Early Paleozoic (Famatinian) deformation in this part of the North Patagonian Massif and the inferred boundary of the Early Paleozoic Cuyania (Precordillera) Terrane north of Patagonia support the interpretation that extra-Andean Patagonia collided with Gondwana South America during the Gondwanide orogeny. It is possible that Patagonia was part of a plate and that the long Gondwanide fold belt represented its collision zone. **INDEX TERMS:** 8015 Structural Geology: Local crustal structure; 8025 Structural Geology: Mesoscopic fabrics; 8102 Tectonophysics: Continental contractional orogenic belts; 9360 Information Related to Geographic Region: South America; 9614 Information Related to Geologic Time: Paleozoic; **KEYWORDS:** Patagonia, structures, thrust tectonics, Gondwana, plates. **Citation:** von Gosen, W., Thrust tectonics in the North Patagonian Massif (Argentina):

Implications for a Patagonia plate, *Tectonics*, 22(1), 1005, doi:10.1029/2001TC901039, 2003.

### 1. Introduction

[2] In southern Argentina, extra-Andean Patagonia represents a geotectonic unit whose history is unclear and has been interpreted in different ways. In 1984, Ramos [1984] postulated that Patagonia represents a terrane which collided with Gondwana South America during the Carboniferous-Early Triassic (Gondwanide) time interval [see also, Ramos, 1986, 1988]. He proposed a SW directed subduction and related the deformational structures in the Sierras Australes of the Buenos Aires Province, north of the inferred suture (Figure 1), to collisional tectonics. In a later model, Sellés Martínez [1989] proposed a collision by sinistral transpressive kinematics, based on the architecture of the Sierras Australes fold-and-thrust belt.

[3] This contrasts with the opinion of Dalla Salda *et al.* [1992a, 1992b, 1993, 1994], who postulated that the belt of Early Paleozoic (Famatinian) deformation and metamorphism in the Sierras Pampeanas of western Argentina continues southward across the boundary into Patagonia. According to this model, Patagonia would have been part of western Gondwana since the Early Paleozoic and did not represent a separated terrane. The Early to Late Paleozoic intrusive activity in northern Patagonia together with acid volcanism has been related to an "Inner Cordilleran Arc," formed during E directed subduction beneath the western margin of Gondwana in the Devonian-Permian interval [e.g., Cingolani *et al.*, 1991; discussion in Rapela and Kay, 1988]. Compressive deformation in northeast Patagonia, Sierras Australes, and Tandilia during the Late Paleozoic has been interpreted in terms of dextral transpression under N-S contraction [e.g., Rossello *et al.*, 1997].

[4] It is well known that Permian to Permo-Triassic magmatic rocks follow a N-S trend in the Cordillera of western Argentina and then turn toward southeast into the area of northern Patagonia [e.g., Linares *et al.*, 1980; Caminos *et al.*, 1988; Kay *et al.*, 1989; López-Gamundi *et al.*, 1995; Llambías, 1999]. Hence, in the east they approximately follow the northern margin of Patagonia. The NW-SE trend of Late Paleozoic magmatics in northern Patagonia has been related to a SW directed subduction by Ramos [1984, 1986].

[5] In the La Pampa Province, north of the inferred terrane suture of Ramos [1984, 1986], evidence for Famatinian deformation, metamorphism, and plutonism has been

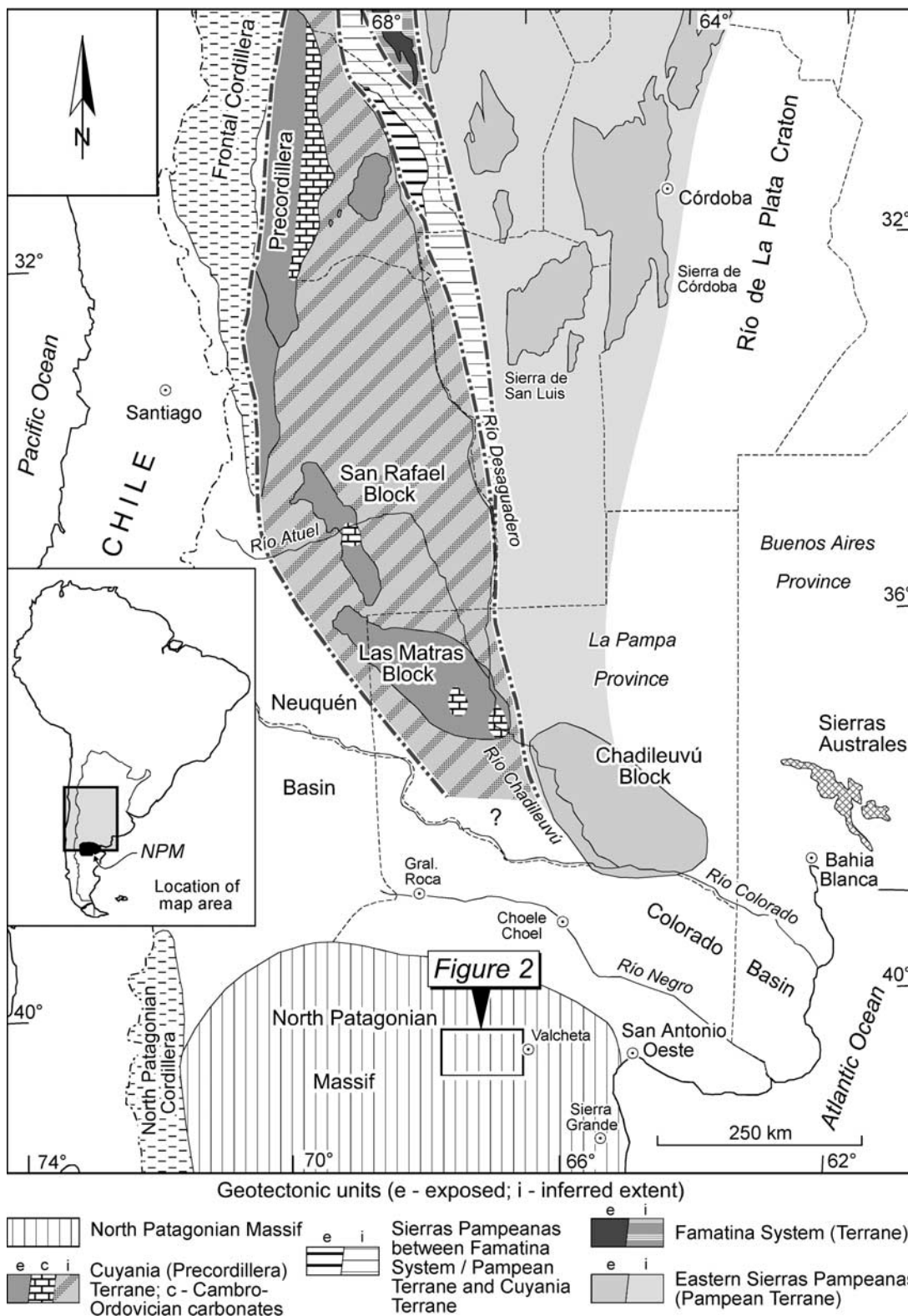


**Figure 1.** Overview map of the main geotectonic units in western and southwestern Argentina, compiled and adapted after von Gosen and Prozzi [1998] and Sato et al. [2000]. Frame depicts location of map of Figure 2. Inset map also shows location of North Patagonian Massif (NPM). Note that Las Matras and Chadileuvú Blocks consist of single scattered outcrops.

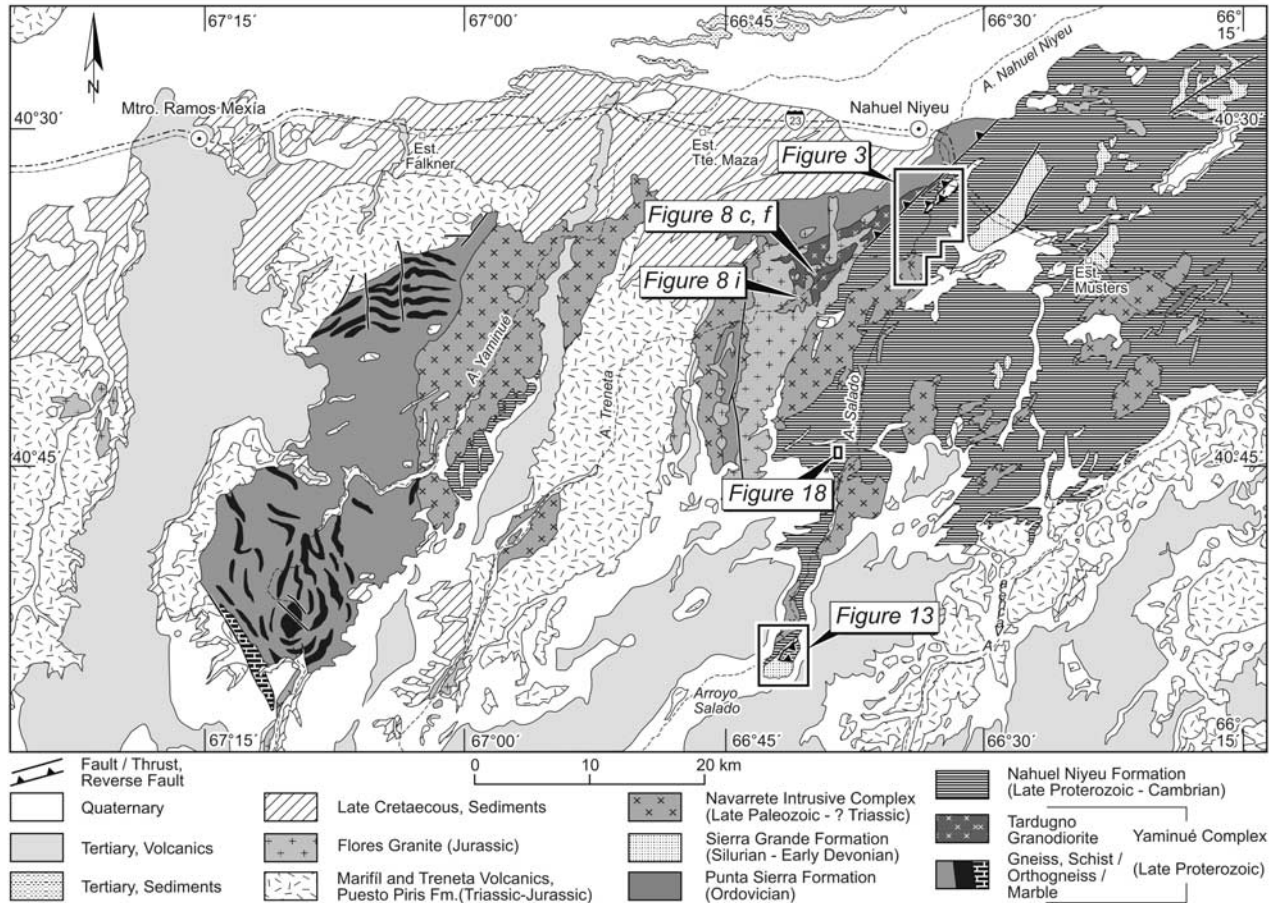


**Figure 2.** Geological sketch map of the area west of Valcheta (North Patagonian Massif), compiled and adapted after *Caminos and Espejo* [1999] and own investigations. For location of map compare Figure 1. Frames and dots show locations of Figures 3; 8c, 8f, 8i; 13; and 18.

reported from scattered exposures in the Chadileuvú Block [Llambías et al., 1996; Tickj et al., 1999a, 1999b; Sato et al., 2000]. To the northwest follows the Las Matras Block (Figure 1) which is characterized by a Grenvillian intrusion [Sato et al., 2000]. It represents the southeastern part of the Cuyania (Precordillera) Terrane with relics of Cambro-Ordovician carbonates in the south [Melchor et al., 1999].

[6] In northern Patagonia, the North Patagonian Massif is located between ~39° and 44°S and the foothills of the Patagonian Cordillera to the west. It represents an area of poorly exposed Precambrian to Early Paleozoic metamorphic rocks along with Early Paleozoic to Jurassic intrusions. A post-Middle Carboniferous uplift and cratonization of the massif was proposed by *Caminos et al.* [1988]. Triassic, Jurassic, and Tertiary volcanics widely cover the older successions [e.g., *Stipanovic and Methol*, 1980]. The northern margin of the massif is marked by the Colorado Basin in the east and the Neuquén Basin in the west (Figure 1). As there are no Paleozoic rocks or ophiolites exposed within this boundary zone at the northern margin of Patagonia, studies in the North Patagonian Massif to the south can give evidence for either a possible terrane collision or a south-

ward continuation of the Famatinian basement from western Argentina into northern Patagonia.

[7] The present study deals with one part of the northeastern segment of the massif. In the area west of the village of Valcheta (Figure 1), two separated study areas give an insight into the deformational history of Early Paleozoic rocks and their relations to different intrusions (Figure 2). As in many parts of this segment of the North Patagonian Massif, however, the outcrop situation is poor. In the text, the structural and metamorphic evolution in both areas is described in separate chapters. This finally will lead to an interpretation of the larger scale tectonics in this part of northern Patagonia and Patagonia's collision with Gondwana South America in the north.

## 2. Lithological Units

[8] In both study areas, the Nahuel Niyeu formation [e.g., *Caminos and Llambías*, 1984; *Chernicoff and Caminos*, 1996b] represents a monotonous succession of phyllites alternating with quartzites on a decimeter to meter scale.

It can directly be compared with the El Jagüelito formation (“Ectinitas El Jagüelito” [Ramos, 1975]) to the southeast in the areas west of Mina Gonzalito and Sierra Grande near the Atlantic coast [e.g., Caminos and Llambías, 1984; Huber-Grünberg, 1990; Giacosa, 1987, 1994, 1999]. Based on a Rb-Sr date of Linares *et al.* [1990] and the age pattern of inherited zircons of the El Jagüelito formation [Pankhurst *et al.*, 2001], a Late Proterozoic to Cambrian age can be estimated for the turbiditic succession.

[9] The phyllitic rocks are intruded by granodiorites to granites of the so-called Punta Sierra formation. Radiometric dating in the area east of Sierra Grande [Varela *et al.*, 1997, 1998] has shown that the intrusive rocks are Early to Mid-Ordovician in age. In the area west of Valcheta, the Tardugno granodiorite, as part of the Yaminué Complex, has been assigned to the Precambrian based on Rb-Sr dating [Caminos *et al.*, 1994]. The same accounts to leukogranites within this complex, which is interpreted as Precambrian basement [Caminos *et al.*, 1994; Chernicoff and Caminos, 1996a] and is also exposed in the southwest. It has been compared with the Precambrian basement rocks southeast of Valcheta (“Gonzalito Block” west of Mina Gonzalito) [e.g., Ramos, 1975; Caminos and Llambías, 1984; Giacosa, 1987; Linares *et al.*, 1990; Caminos *et al.*, 1994; Varela *et al.*, 1998].

[10] The shallow marine clastic succession of the Sierra Grande formation consists of quartzitic sandstones and siltstones with some conglomerate layers but without any carbonates. Based on a few fossil findings in the area of Sierra Grande, these deposits are interpreted to be Silurian to Early Devonian in age [e.g., Braitsch, 1965; Müller, 1965; Castellaro, 1966; Amos, 1972; Limarino *et al.*, 1999]. There, they unconformably overlie either the intrusions of the Punta Sierra formation or the simply deformed and metamorphosed phyllite succession of the El Jagüelito formation.

[11] The area west of Valcheta is characterized by widely distributed intrusions which are assigned to the Navarrete Intrusive Complex (Figure 2). It consists of granodiorites and granites with a possible Late Paleozoic to Triassic age (probably Permian [Caminos, 1999]). A porphyric granite in the Arroyo Salado area south of Nahuel Niyeu is interpreted as the youngest intrusion of the complex [Caminos, 1999]. The intermediate to acid Triassic Treneta volcanics, Jurassic volcanics of the Marifil Group, and Tertiary basalts cover wide areas. The Flores granite, which has been dated as Jurassic [Pankhurst *et al.*, 1993], shows that volcanism was accompanied by intrusive activity.

### 3. Structure

#### 3.1. Northern Segment

[12] The northern segment covers an area south of the village of Nahuel Niyeu around the Arroyo Nahuel Niyeu and further to the south (Figures 2 and 3). It has been mapped and structurally analyzed by Chernicoff and Caminos [1996b]. Their results and interpretations, however, in many parts differ from those presented here. The deformations and structures within the different units are described

from north to south, in accordance with the relative chronology found in the field.

[13] The internal deformation of the phyllites and quartzites of the Nahuel Niyeu formation is characterized by a penetrative  $S_1$  foliation which is parallel to bedding planes ( $S_0$ ) and sporadically cuts across under small angles. Hence, a reconstruction of first fold structures ( $F_1$ ) was not possible. Equivalents of  $S_1$  foliation planes do not occur in the younger lithological units.

[14] On a microscale, the  $S_1$  foliation is recorded by aligned sericite and  $\pm$ chlorite and contains quartz, plagioclase, and k-feldspar clasts. Thin quartz veins are parallel to  $S_1$  planes where no indications for a crenulated older foliation could be detected. Quartz occurs in single, small grains within the sericite matrix and is recrystallized syn- to post- $D_1$ . Larger polycrystalline quartz consists of coarse recrystallization grains with straight grain boundaries meeting at triple junctions. Comparable fabrics occur in quartz veins. The microfabrics suggest a slight greenschist facies metamorphism which outlasted  $D_1$  under static conditions. Equivalent structures were also found in the Arroyo Salado area to the south and outcrops west of Valcheta and can broadly be attributed to Cambrian tectonism.

#### 3.1.1. Initial Thrusting and Related Structures

##### 3.1.1.1. Nahuel Niyeu Thrust Sheet

[15] In the area south of Nahuel Niyeu, the Nahuel Niyeu formation is displaced as Nahuel Niyeu Thrust Sheet over the Sierra Grande formation in the south (Figure 3). There, two thrust faults have been described by Chernicoff and Caminos [1996b]. Detailed mapping over a distance of several kilometers has shown, however, that only one thrust (as depicted by Caminos and Espejo [1999]) follows a variable NE-SW trend. It is referred to here as Nahuel Niyeu Thrust (Figures 4a and 4b). In distinct parts the strike changes to W-E or NNE-SSW. The further continuation of the thrust to the northeast and southwest is unclear due to a younger cover.

[16] In both segments of the Nahuel Niyeu Thrust, east and west of Arroyo Nahuel Niyeu, tight  $F_2$  folds on decimeter to meter scale at the base of the thrust sheet (Figure 5a) record S- and Z-geometries. These indicate a larger-scale folding related to thrust tectonics (Figure 6). Further up-section, in the hanging wall phyllites, only single  $F_2$  fold structures could be found.  $B_2$  axes have variable NE-SW to NW-SE orientations. Gliding of the Nahuel Niyeu Thrust Sheet over the Sierra Grande formation took place parallel to  $S_2$  foliation planes at the base (Figure 5b). They are parallel to  $S_1$  planes and up-section represent axial-plane cleavage planes associated with  $F_2$  folds. In the hanging wall parts of the Nahuel Niyeu formation only single  $C_2$  shear planes could be found. In the Sierra Grande formation of the footwall, displacements took place parallel to bedding planes ( $S_0$ ). West of Arroyo Nahuel Niyeu, however,  $S_2$  planes at the base of the thrust sheet partly cut across bedding of the Sierra Grande formation (Figure 4b).

[17] The transport direction of the Nahuel Niyeu Thrust Sheet is indicated by single S/C fabrics and asymmetric quartz  $\sigma$ -clasts at the base as well as slickensides on bedding planes and/or  $C_1$  shear planes within the Sierra Grande

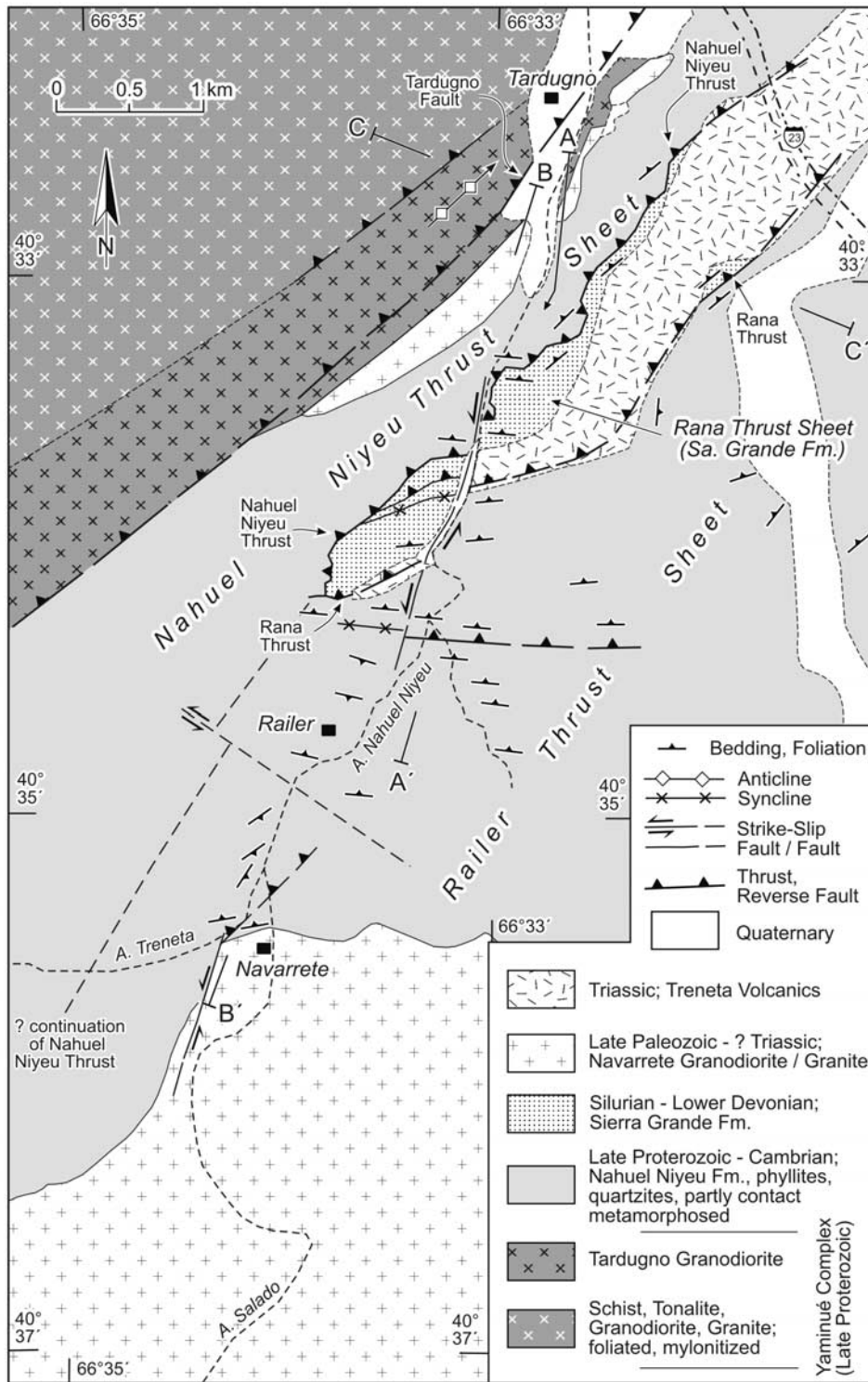


**Figure 3.** Tectonic sketch map of the area of the Arroyo Nahuel Niyeu south of Nahuel Niyeu (for location compare Figure 2). Map compiled and adapted after *Chernicoff and Caminos* [1996b] and own structural field mapping.

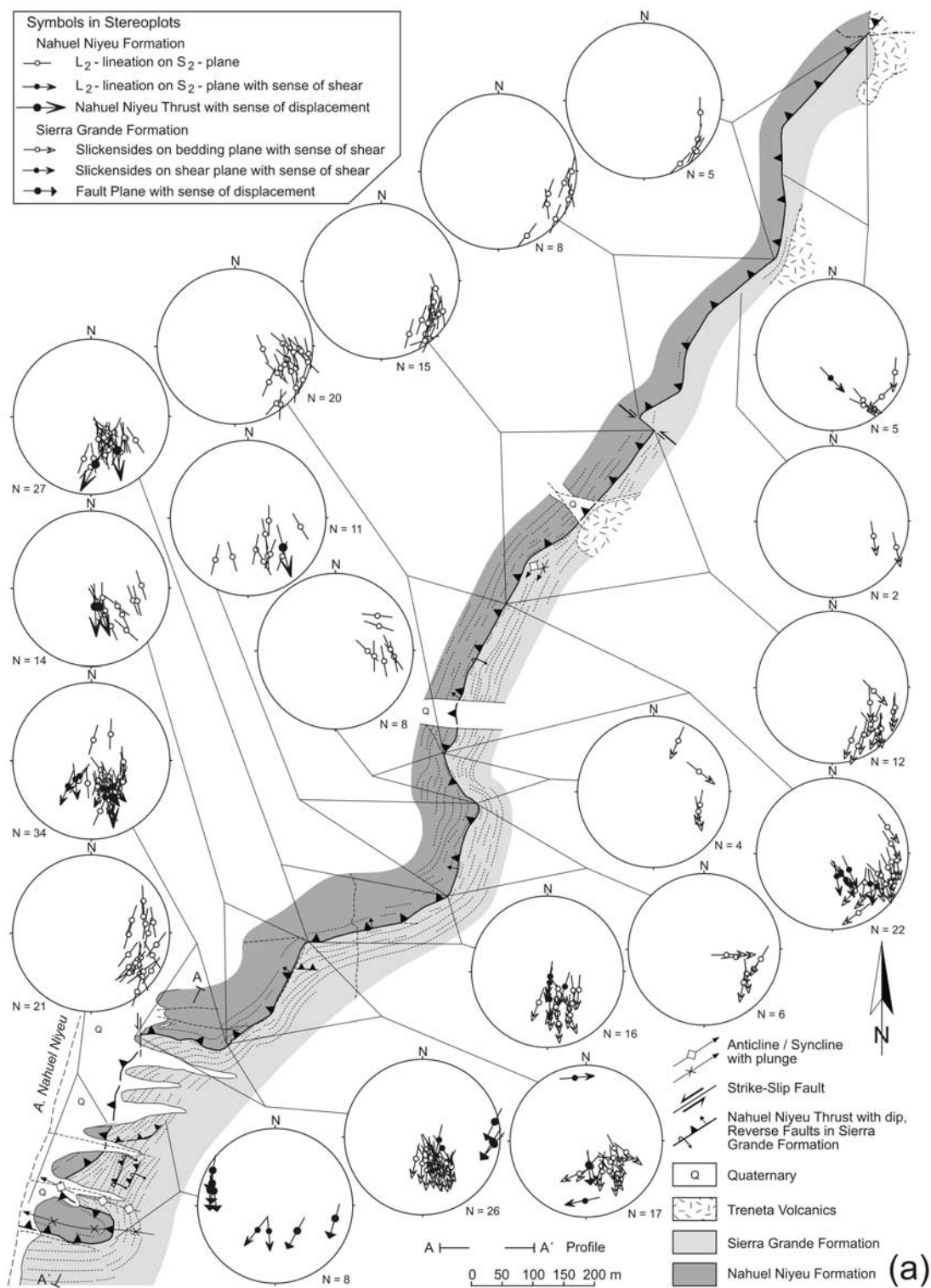


**Figure 4.** Sketch maps of the Nahuel Niyeu Thrust east (a) and west (b) of Arroyo Nahuel Niyeu with southwestern segment of Rana Thrust in (b) (based on structural field mapping). In the lower hemisphere, equal-area Hoepfener plots [Hoepfener, 1955] the lineation is projected on the pole of the related plane. Arrows indicate the relative sense of shear/displacement of the hanging wall units.

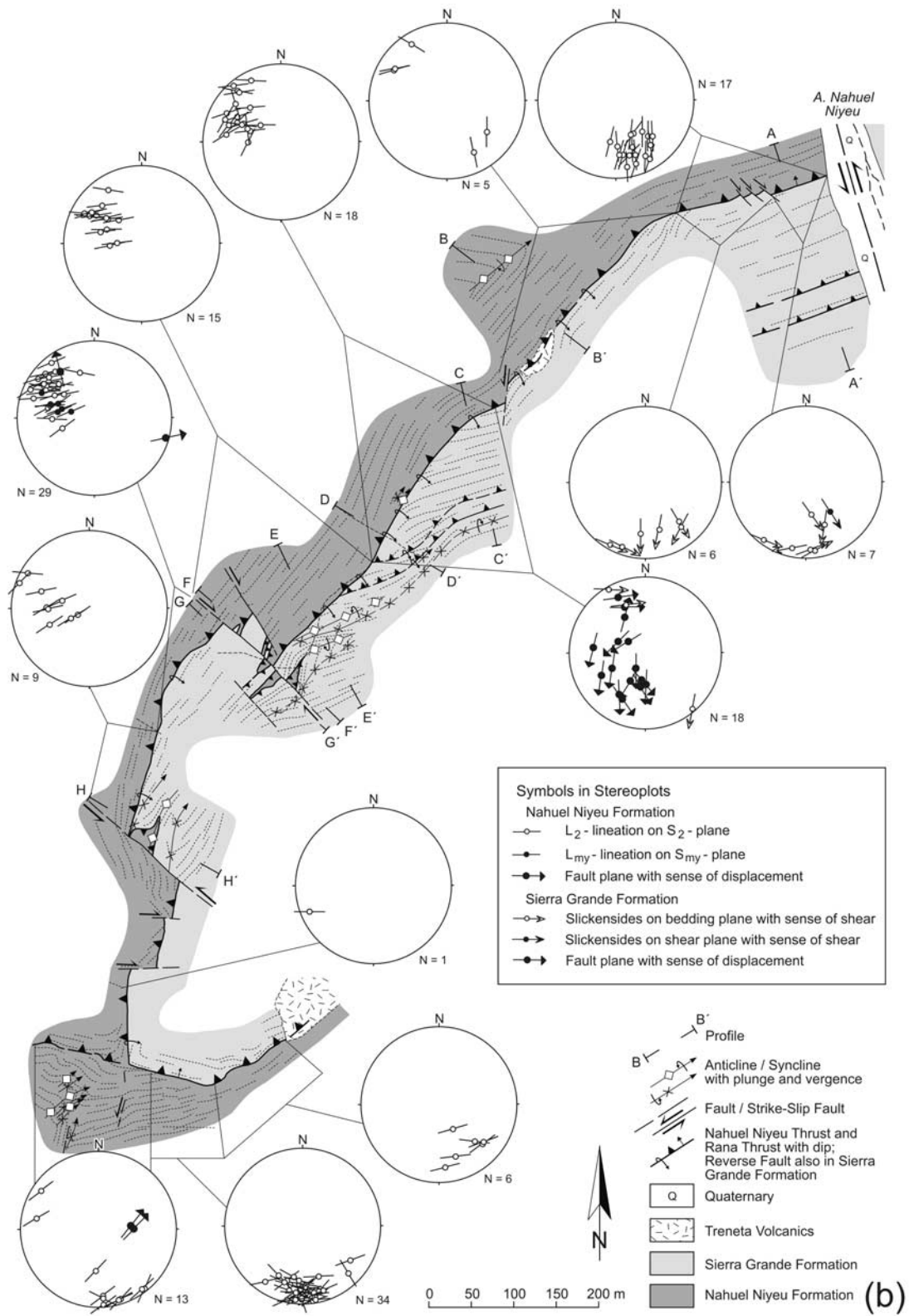
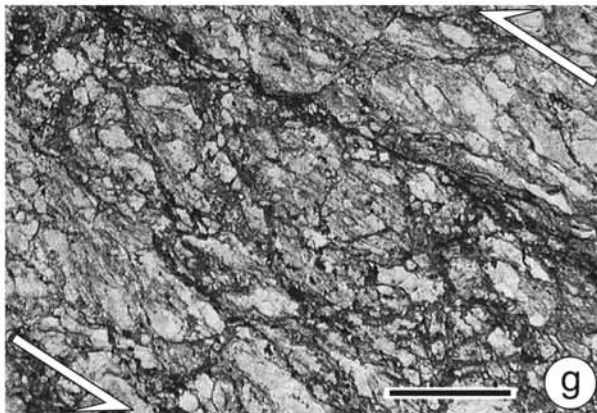
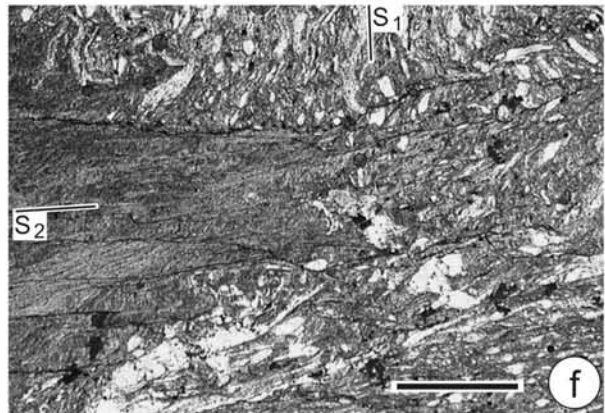
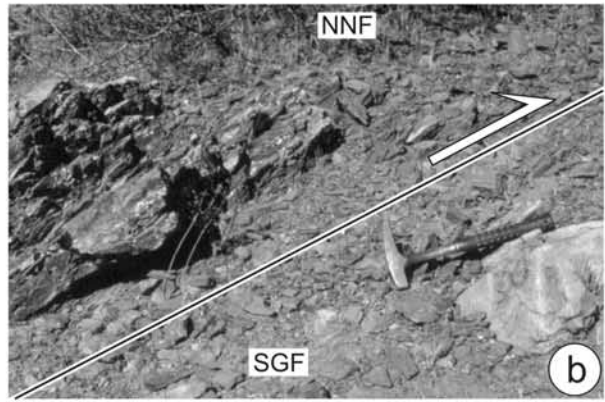
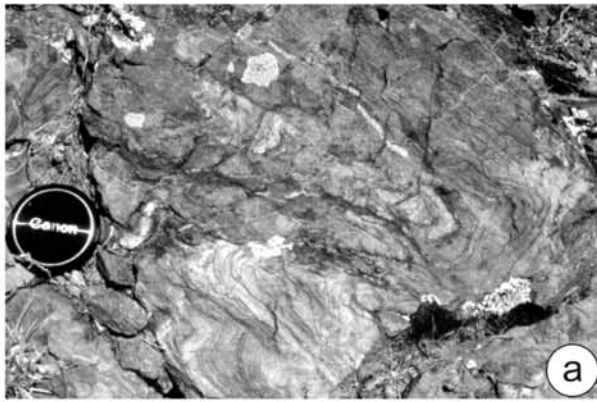


Figure 4. (continued)



formation of the footwall. The general trend shows a S directed thrusting east of Arroyo Nahuel Niyeu which changes to a SW directed transport west of the river (Figures 4a and 4b). This is also supported by the orientations of  $L_2$  lineations on  $S_2$  foliation planes within the basal parts of the phyllites. They are recorded by aligned sericite and display a  $\sim$ N-S to  $\sim$ NE-SW orientation. Deviations from this trend are related to NE-SW to N-S striking parts of the thrust where the plane steeply dips to the W or is even overturned. This situation is due to a younger deformational event which overprinted the Nahuel Niyeu Thrust Sheet stacked over the Sierra Grande formation (see below).

[18] Thrusting is accompanied by the formation of  $F_2$  folds on a decimeter to meter scale and with different vergences. They only occur at the base of the thrust sheet with axes always parallel to the  $L_2$  lineation and are partly combined with a crenulation cleavage (Figure 5c). The folds are interpreted to be related to intense stretching during thrust tectonics.

### 3.1.1.2. Tardugno Granodiorite

[19] The Tardugno granodiorite SW of Puesto Tardugno (Figure 3) is overprinted by a heterogeneously developed foliation which passes into a mylonite foliation ( $S_{my}$ ). Such mylonites, described by *Chernicoff and Caminos* [1996a], were also found in the southwestern along-strike continuation near the Arroyo Treneta (Figure 2). In both areas, feldspar  $\sigma$ -clasts, single S/C fabrics, and shear bands demonstrate a relative sense of shear of the hanging wall toward SSW to SW (Figures 7a, 8a, and 8c).

[20] West of Puesto Tardugno, intensely foliated and mylonitized granodiorites, granites, leukogranites, and some schists have been assigned to the Precambrian Yaminué Complex by *Chernicoff and Caminos* [1996a, 1996b]. The granodiorites can directly be compared with the Tardugno granodiorite. This also applies to their intense deformation. Hence, it is assumed here that these intrusive rocks represent an intrusive complex. They are partly mylonites with kinematic indicators recording a top-to-WSW sense of shear (Figure 8b). The schists are intensely foliated together with

the granitoids and probably represent their country rocks with a Precambrian age [see also *Chernicoff and Caminos*, 1996a].

### 3.1.1.3. Rana Thrust Sheet

[21] In the north, the Sierra Grande formation is overthrust by phyllites and quartzites of the Nahuel Niyeu Thrust Sheet. In its southwestern part (Figure 7b), single outcrops show that the Sierra Grande formation is thrust along a steeply north dipping thrust fault southward over phyllites and quartzites of the Nahuel Niyeu formation. This thrust at the base of the Sierra Grande formation shall be named Rana Thrust.

[22] Toward northeast, the basal parts of the Sierra Grande formation are exposed in the Arroyo Nahuel Niyeu. In the big cliff, quartzitic sandstones are affected by south directed thrusting with the formation of duplex structures (Figures 9a and 9b). The intense deformation also shows that the Sierra Grande formation does not overlie the phyllite succession of the Nahuel Niyeu formation in the south along a basal sedimentary contact but was overthrust along the Rana Thrust. This is furthermore supported by single outcrops in the northeastern segment of the Rana Thrust (east of Arroyo Nahuel Niyeu) where the sandstones tectonically overlie the phyllites. Hence, the Sierra Grande formation succession in the footwall of the Nahuel Niyeu Thrust represents a separate thrust sheet, introduced here as Rana Thrust Sheet, which is widely covered by Triassic volcanics (Figure 3).

[23] The internal deformation of the Rana Thrust Sheet is different in both segments east and west of Arroyo Nahuel Niyeu. In the east, the succession homoclinally dips to the N to NW. Just east of Arroyo Nahuel Niyeu it is folded together with the overthrust phyllites of the Nahuel Niyeu Thrust Sheet (Figures 6a, 6b, and 10: profile A–A'). West of the river, the Rana Thrust Sheet is bent around a large, south vergent syncline structure (Figure 10: profile B–B'). The southern part of its southern limb is bent around an anticline and crosscut by the above north dipping thrusts and duplexes linked to the Rana Thrust at the base (Figure 9). The northern limb of the syncline is crosscut by north

**Figure 5.** (opposite) (a) View toward approximately west on tight  $F_2$  fold in phyllites of the Nahuel Niyeu formation at the base of the Nahuel Niyeu Thrust Sheet and within open syncline structure of Figure 6a (southernmost part of Nahuel Niyeu Thrust Sheet east of Arroyo Nahuel Niyeu,  $\sim$ 2.25 km south of Puesto Tardugno). (b) View toward approximately NE on Nahuel Niyeu Thrust. Penetratively foliated ( $S_2$ ) quartzitic phyllites of the Nahuel Niyeu formation (NNF, Nahuel Niyeu Thrust Sheet) are thrust southward over sandstones of the Sierra Grande formation (SGF) (east of Arroyo Nahuel Niyeu,  $\sim$ 1.9 km south of Puesto Tardugno). (c) View toward approximately NE on limb of  $\sim$ SE vergent  $F_2$  fold structure. Folding is combined with an approximately NW dipping  $S_2'$  crenulation cleavage (phyllite in basal part of Nahuel Niyeu Thrust Sheet, east of Arroyo Nahuel Niyeu,  $\sim$ 1.5 km SSE of Puesto Tardugno). (d) View toward NE along outcrops of cataclasite to breccia of the Tardugno fault (northwestern margin of Arroyo Nahuel Niyeu,  $\sim$ 460 m SSW of Puesto Tardugno; outcrops are  $\sim$ 3 m high). (e) View toward south on  $F_3$  folds in phyllites at the base of the Nahuel Niyeu Thrust Sheet recording opposite vergences (east of Arroyo Nahuel Niyeu, location as in (b)). (f) Photomicrograph of  $F_2$  hinge zone in phyllite of the Nahuel Niyeu formation beneath the Rana Thrust. The  $S_1$  foliation is crenulated between axial-plane  $S_2$  cleavage planes (southwestern part of Railer Thrust Sheet west of Arroyo Nahuel Niyeu,  $\sim$ 0.9 km north of Puesto Railer). (g) Photomicrograph of foliated cataclasite (phyllite) at the base of the Nahuel Niyeu Thrust Sheet. S/C fabrics depict a top-to-south sense of shear (east of Arroyo Nahuel Niyeu, location as in (a)). (h) Photomicrograph of S/C fabrics in sheared sandstone of the Sierra Grande formation just beneath the Nahuel Niyeu Thrust. The south directed sense of shear of the hanging wall is comparable to that in the sheared phyllites above (compare (f)); east of Arroyo Nahuel Niyeu, location as in (b)). In (f), (g), and (g) - Scale bars are 1 mm long, plane polarized light.

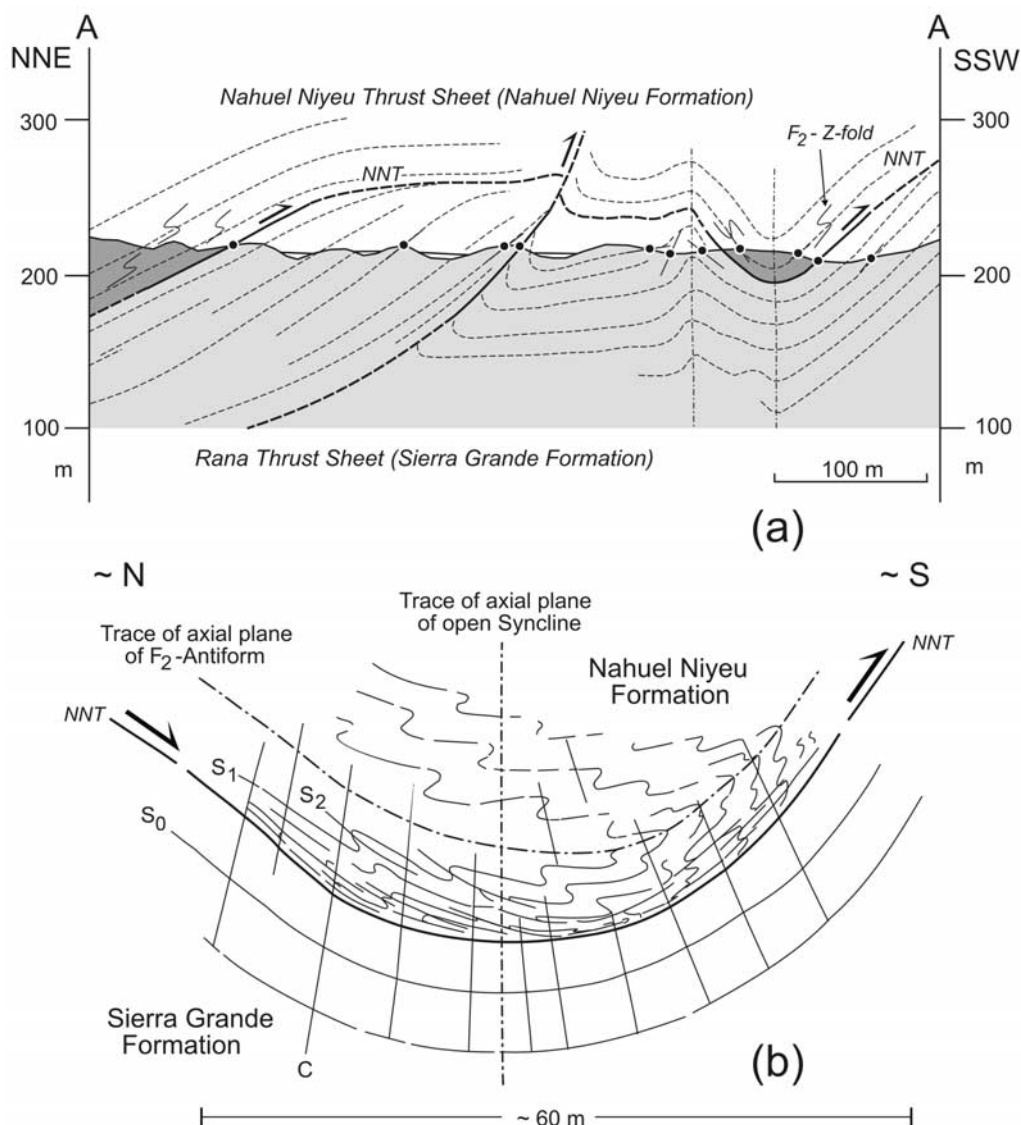


**Figure 6.** (a) Profile across the Nahuel Niyeu Thrust (NNT) just east of Arroyo Nahuel Niyeu (for location compare Figure 4a). Depicted  $F_2$  Z-folds are schematic. (b) Simplified and schematic profile cartoon across the open syncline in the southern part of (a). Note bending of the Nahuel Niyeu Thrust along with the thrust sheet and underlying Sierra Grande formation.  $F_2$  folding is intensified toward the base of the thrust sheet and the fold geometries permit to infer an  $F_2$  antiform related to approximately south directed thrusting.

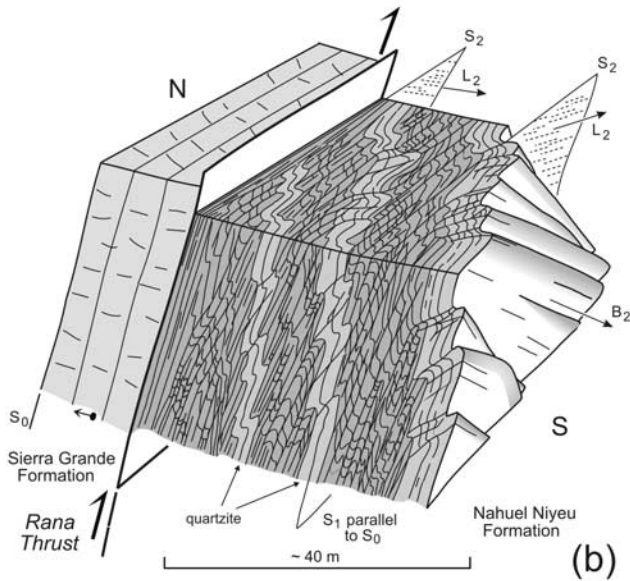
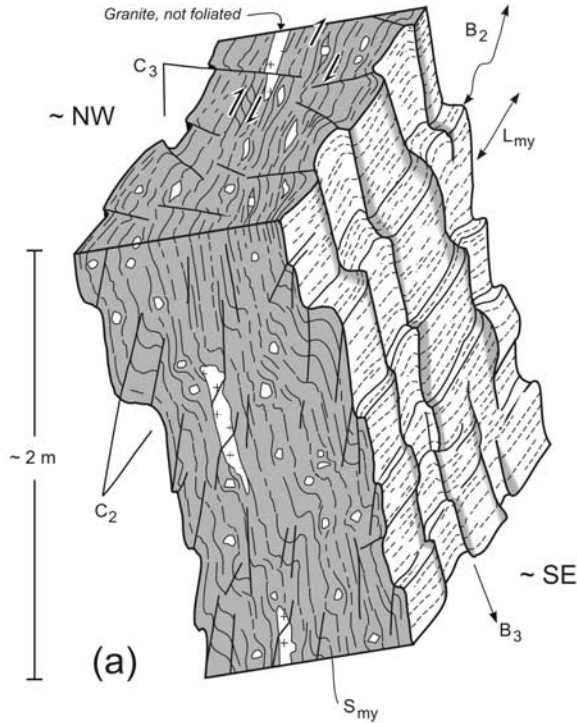
dipping thrust faults. They separate a thin slice of steeply north dipping sandstones in normal position (cross-bedding) from a subvertical to steeply northward overturned succession beneath the Nahuel Niyeu Thrust.

[24] In particular the situation west of Arroyo Nahuel Niyeu shows that the southward directed displacement of the Nahuel Niyeu Thrust Sheet was combined with folding and thrusting within the Rana Thrust Sheet. It led to S directed thrusting of the Sierra Grande formation (Rana Thrust Sheet) over the Nahuel Niyeu formation along the Rana Thrust in the south. The differences in the internal deformation and lateral shortening within the Rana Thrust Sheet are related to a ~N-S striking strike-slip fault within

the Arroyo Nahuel Niyeu (Figure 3) which is not exposed. It sinistrally displaces both blocks along with the bounding thrust faults and is interpreted as a transfer (tear) fault relative to thrust tectonics.

#### 3.1.1.4. Railer Thrust Sheet

[25] Beneath the Rana Thrust in the southwest, phyllites of the Nahuel Niyeu formation are affected by  $F_2$  folding on a centimeter to several meters scale.  $F_2$  folds are associated with an  $S_2$  crenulation cleavage which becomes penetrative toward the Rana Thrust and is related to the displacement (Figure 7b). A comparable situation was found in the northeastern part of the Rana Thrust where



phyllites in the footwall are intensely folded around  $F_2$  structures.

[26] The situation at the southern boundary of the Rana Thrust Sheet shows that the Sierra Grande formation has been cut out of the sedimentary succession in the subsurface. The sediments were carried along the Rana Thrust southward over the older phyllites plus quartzites (Nahuel Niyeu formation). This suggests that the former, southern subsurface continuation of the Sierra Grande formation lies beneath the phyllites of the Nahuel Niyeu formation. As a consequence, the southern succession of phyllites and quartzites is not autochthonous but should represent an important thrust sheet which has overridden the Sierra Grande formation sediments in the subsurface. This displaced unit shall be named Railer Thrust Sheet although its basal thrust is not exposed (Railer Thrust).

[27] The internal deformation of the phyllites in the Railer Thrust Sheet is indicated by single S to SW vergent  $F_2$  folds on a decimeter to meter scale, partly with curved  $B_2$  axes. East of Arroyo Nahuel Niyeu, the homoclinally north dipping phyllites are crosscut by a north dipping thrust fault (Figures 3 and 10: profile A–A'). Slickensides indicate a S to SSW directed displacement of the hanging wall. West of the river,  $S_2$  planes of the phyllites steeply dip beneath the Rana Thrust. Toward the south, the  $S_1$  foliation is bent around an open  $F_2$  syncline structure (Figure 10: profile B–B'). Its geometry is supported by the orientations and vergences of associated smaller  $F_2$  folds.

**3.1.2. Deformations After Thrusting**

[28] South of Puesto Tardugno, the Nahuel Niyeu Thrust Sheet is crosscut along a NE-SW striking fault, described by *Caminos and Llambías* [1984] and *Chernicoff and Caminos* [1996b]. It is introduced here as Tardugno fault (Figure 3). Single outcrops at the river expose an ~20 m thick cataclasite to breccia horizon (Figure 5d). It consists of pieces and crushed rocks of the foliated and mylonitized Tardugno granodiorite exposed at both sides of the fault. Furthermore, isolated clasts of the Navarrete granodiorite to

**Figure 7.** (opposite) Simplified, schematic, and composite block sketches. (a) Structures in mylonite of the Tardugno granodiorite from steeply SE dipping limb of  $F_2$  antiformal structure northwest of Tardugno fault (~550 m SSW of Puesto Tardugno). Feldspar  $\sigma$ -clasts and S/C fabrics indicate a dextral sense of shear parallel to the mylonite lineation ( $L_{my}$ ). The light granite within the mylonite foliation ( $S_{my}$ ) is not foliated and probably belongs to the Navarrete Intrusive Complex. The  $S_{my}$  foliation is folded around  $F_2$  and  $F_3$  folds which are combined with  $C_2$  and  $C_3$  shear planes, respectively. (b) Structures at the southwesternmost part of the Rana Thrust (west of Arroyo Nahuel Niyeu, ~0.9 km north of Puesto Railer). The Sierra Grande formation sandstones of the Rana Thrust Sheet are thrust southward over phyllites with quartzite layers of the Nahuel Niyeu formation (Railer Thrust Sheet). The phyllitic succession is folded around  $F_2$  crenulation folds combined with an  $S_2$  crenulation cleavage. The latter becomes penetrative toward the thrust.

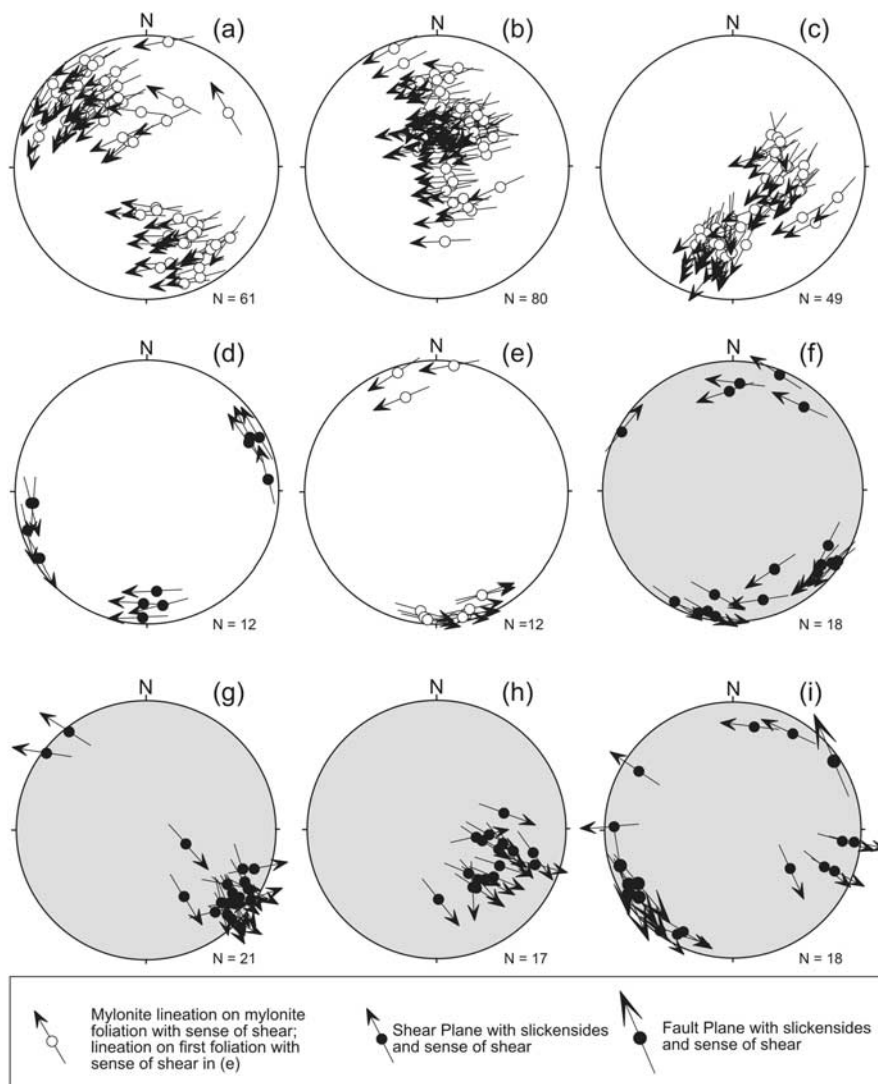


**Figure 8.** Lower hemisphere, equal-area Hoeppener plots [Hoepfner, 1955] of kinematic indicators in Tardugno granodiorite ((a)–(f)), with granites and schists in (b)), Navarrete granodiorite to granite ((h) and (i)), and cataclasite of Tardugno fault (g). Data of (c), (f), and (i) are from locations at Arroyo Treneta (compare Figure 2). The other diagrams are based on data from the area of Arroyo Nahuel Niyeu: (a) and (b) - west of Tardugno fault, (d), (e) and (h) - east of Tardugno fault. White plots - mylonite foliation and mylonitic shear planes; gray plots - younger shear planes in Tardugno granodiorite and first deformational structures in Navarrete granodiorite to granite. In the Hoeppener plots, arrows indicate the relative sense of shear/displacement of the hanging wall unit.

granite on a centimeter to decimeter size occur. They do not record any indication for ductile deformation prior to faulting. Within the strip of cataclasites, slickensides on shear planes demonstrate a reverse, SE directed uplift of the northwestern block along the Tardugno fault [see also Chernicoff and Caminos [1996b] (present Figure 8g). Toward northwest, loose blocks of a second breccia to cataclasite horizon were found within the Tardugno granodiorite. They presumably belong to a second, also NE-SW striking reverse fault with an assumed uplift of the northwestern block. The latter consists of different intrusive rocks and schists of the Yaminué Complex (Figure 3).

[29] Uplift of the northwestern block along the Tardugno fault is attributed to NW-SE compression. It led to the formation of open  $F_2$  folds around  $\sim$ NE-SW striking axes within the mylonites of the Tardugno granodiorite and Yaminué Complex. SW of Puesto Tardugno, the heterogeneously foliated and mylonitized granodiorite is bent around a large-scale, NE-SW striking  $F_2$  antiform (Figures 3 and 10: profile C–C'). Again, this suggests that this deformation is younger than the displacement of the Nahuel Niyeu Thrust Sheet and shearing in the granodiorite.

[30] During  $\sim$ NW-SE compression, the eastern and western segments of the Nahuel Niyeu Thrust were steepened

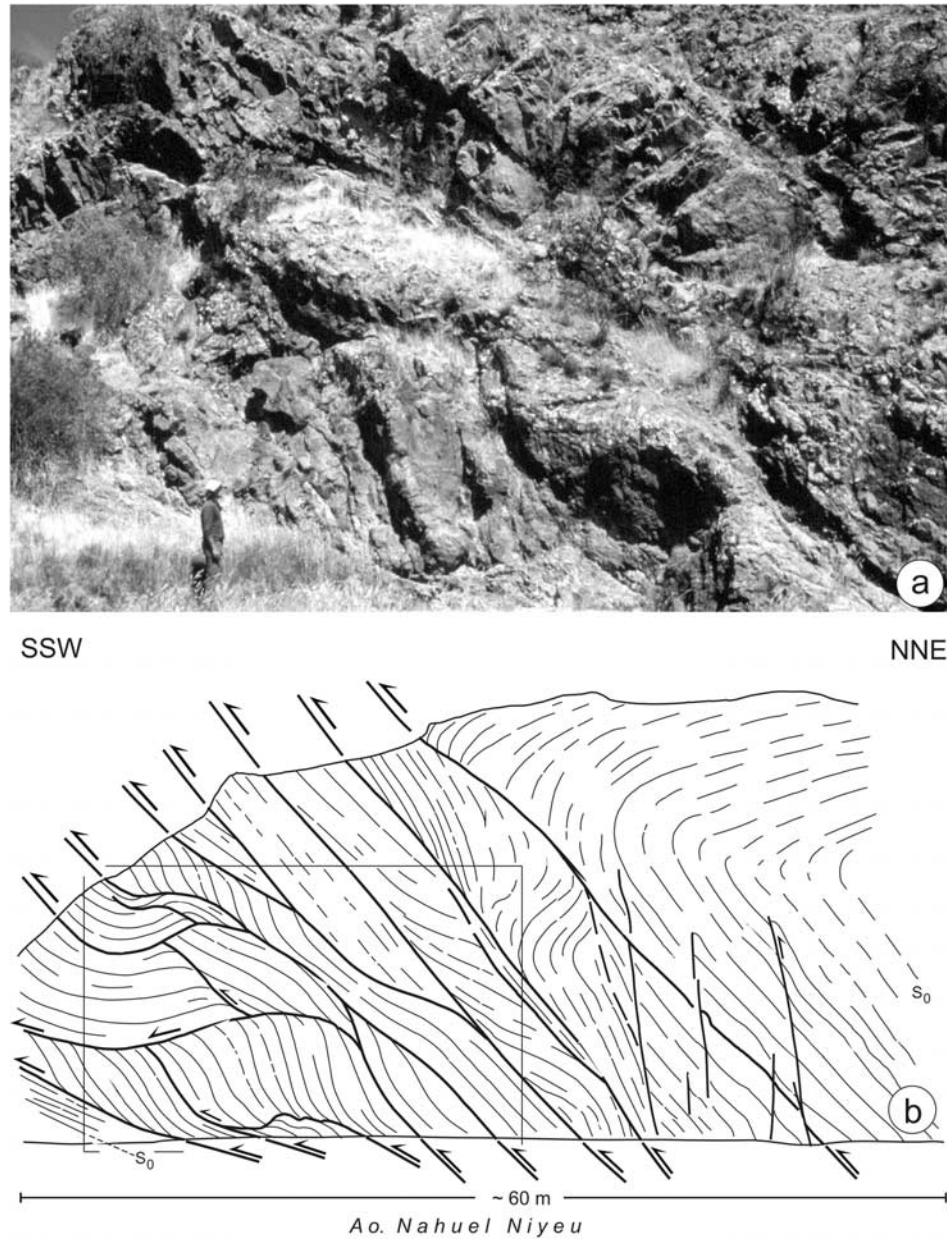


**Figure 9.** Intensely deformed sandstones of the Sierra Grande formation at the base of the Rana Thrust Sheet just above the Rana Thrust (a). Note approximately SSW directed thrusting with the formation of duplex structures. Frame in simplified sketch of the outcrop (b) shows the location of the photograph of (a) (cliff at the western margin of Arroyo Nahuel Niyeu, southern boundary of the Sierra Grande formation, ~1.3 km NNE of Puesto Railer).

and partly overturned (Figures 4a and 4b).  $F_3$  folds around ~NE-SW striking axes and with changing vergences overprint the overthrust phyllite succession on a decimeter to tens of meters scale (Figure 5e). In the western part, the Nahuel Niyeu Thrust is bent into a subvertical to slightly overturned position (compare Figure 11). Further to southwest, the thrust plane and Sierra Grande formation of the Rana Thrust Sheet in the footwall are folded around approximately NE-SW to NNE-SSW striking axes and are displaced along approximately NW directed high-angle

reverse faults. Faulting is combined with folding and younger than the displacement along the Nahuel Niyeu Thrust. In some parts, compression led to the formation of imbricates which seem to have developed from fold structures.

[31] Folding of the Nahuel Niyeu Thrust Sheet as well as the overridden Sierra Grande formation is combined with the formation of ~N-S to W-E striking sinistral and dextral strike-slip faults (Figure 4b) which are interpreted as transfer faults. Strike-slip displacements affected the tectonically

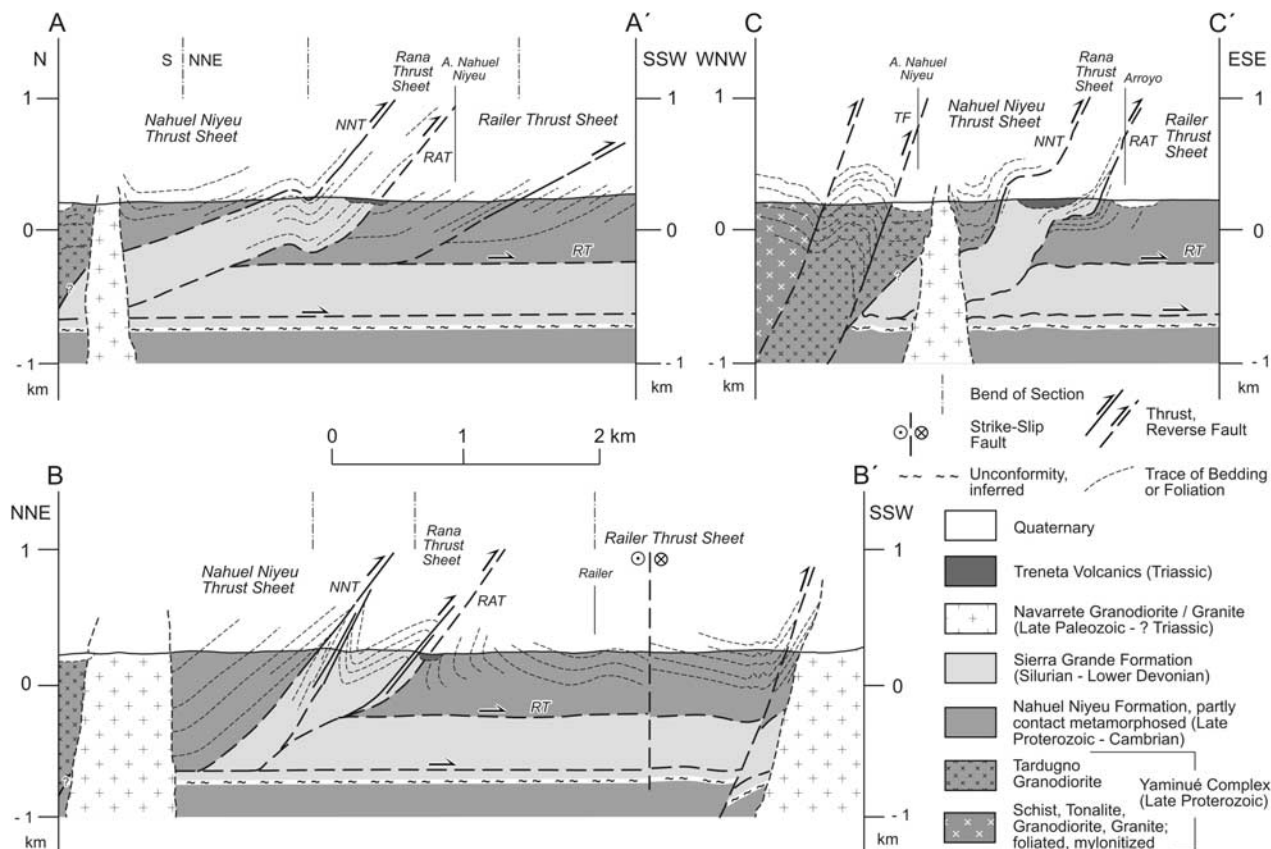


**Figure 10.** Interpretative profiles across the different tectonic units in the area south of Nahuel Niyeu (for locations compare Figure 3). Subsurface geometries are inferred (e.g., depths of décollement horizons). See text for explanations. NNT - Nahuel Niyeu Thrust; RAT - Rana Thrust; RT - Railer Thrust; TF - Tardugno fault.

stacked units and caused the different style of deformation and amount of shortening within adjacent blocks (compare Figure 11). Reverse shear planes and dextral shear zones in combination with reverse shear planes, found within the Navarrete granodiorite east of the Tardugno fault (Figure 8h) and granodiorite at Arroyo Treneta (Figure 8i), respectively, represent first deformational structures in the pluton and can be related to this NW-SE compression.

[32] In the phyllites of the Railer Thrust Sheet  $F_3$  fold structures around  $\sim$ NE-SW striking axes and with changing vergences also occur. They are condensed in the northwestern part of the thrust sheet beneath the Rana Thrust (Figure 4b) and in the southern part, north of the intrusive contact of the Navarrete granodiorite. In the latter locality, intense folding affects the contact metamorphosed phyllites and is presumably combined with a NE-SW striking reverse fault (Figures 3 and 10: profile B-B'). In general, folding was the result of approximately NW-SE compression and can directly be compared with equivalent structures in the Rana and Nahuel Niyeu Thrust Sheets.

[33] Structures of the following approximately W-E compression document the youngest stage of deformation. These are folds on a decimeter to several meters scale. Their axes vary in strike around the N-S direction. The

approximately east or approximately west vergent  $F_4$  folds were found in the phyllites of the Nahuel Niyeu Thrust Sheet and Railer Thrust Sheet. Furthermore, they occur in the mylonites of the Tardugno granodiorite where they overprint older  $F_2$  structures as  $F_3$  folds.

### 3.1.3. Microfabrics

#### 3.1.3.1. Nahuel Niyeu Formation

##### 3.1.3.1.1. $D_2$ - $D_3$ Deformation

[34] At the base of the Nahuel Niyeu Thrust sheet and in the Railer Thrust Sheet beneath the Rana Thrust, the  $S_1$  foliation is crenulated between  $S_2$  cleavage planes on a microscale (Figure 5f). Incompetent layers are foliated. Sericite and chlorite growth syn- to post- $S_2$  is shown by partly polygonal hinges of crenulations and new sericite + chlorite aligned parallel to  $S_2$ . Quartz clasts are ductilely deformed recording more lens-shaped outlines within the  $S_2$  foliation and sericite-chlorite beards in pressure shadows. In the matrix, dynamically generated recrystallization grains occur with submicroscopical sizes whereas feldspar clasts are brittlely deformed. In some mylonitic parts, the penetrative foliation is indicated by aligned sericite with quartz

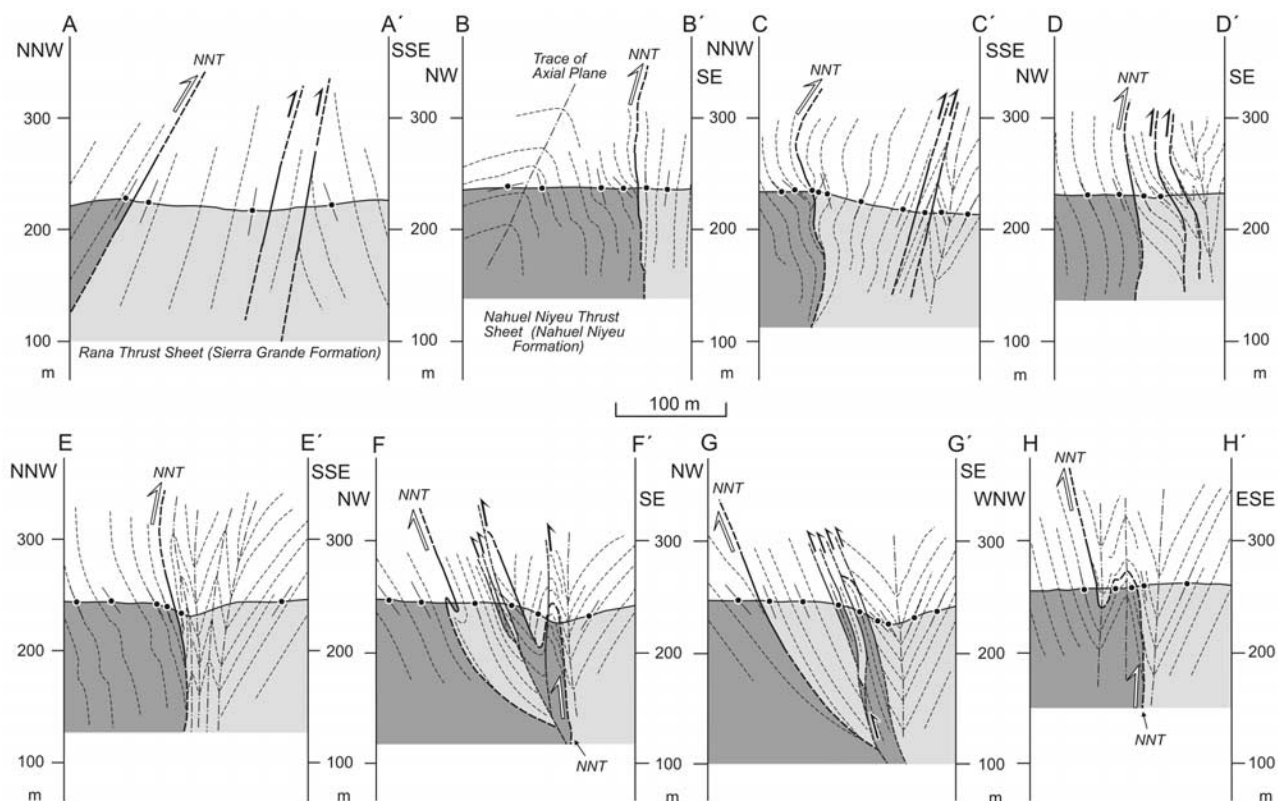


**Figure 11.** Simplified profiles across the Nahuel Niyeu Thrust (NNT) west of the Arroyo Nahuel Niyeu (see Figure 4b for locations). Note that the Nahuel Niyeu Thrust from northeast (profile A–A') to southwest (profile H–H') steepens and finally is overturned. This is related to subsequent compression which led to bending and folding of the inactive thrust. SE dipping high-angle reverse faults cut across the thrust and led to the formation of thin imbricate slices.

( $\pm$ plagioclase,  $\pm$ k-feldspar) clasts in between. The margins of quartz clasts are partly replaced by dynamically generated recrystallization grains.

[35] At the base and in the upper parts of the phyllite succession, S/C fabrics, some asymmetric quartz  $\sigma$ -clasts,  $\sigma$ -shapes of quartz-filled pressure shadows at feldspar clasts, a few shear bands, and displaced feldspar fragments demonstrate a top-to-SW sense of shear parallel to  $L_2$ .

[36] Dynamic quartz recrystallization continued during  $F_2'$  folding along with internal strain (bending, kinking, subgrain formation) and pressure solution at contacts of clastic grains and grain aggregates. Single  $C_2$  shear planes are depicted by reoriented and newly grown sericite. Within sericite + chlorite-rich layers, phyllosilicates are crenulated giving rise to a developing  $S_2$  cleavage. Polygonal hinges of crenulations and random growth in the matrix show that sericite growth outlasted  $D_2$  due to a slight greenschist facies metamorphic overprint.

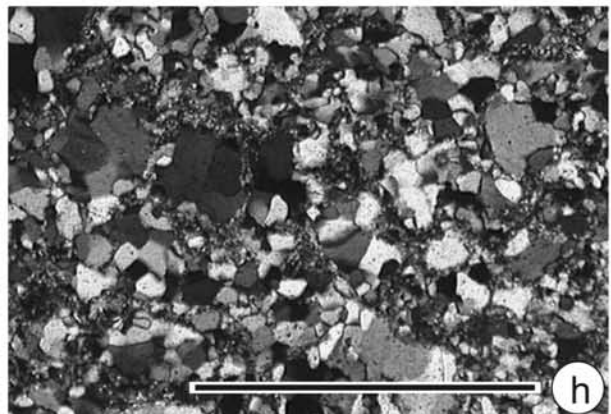
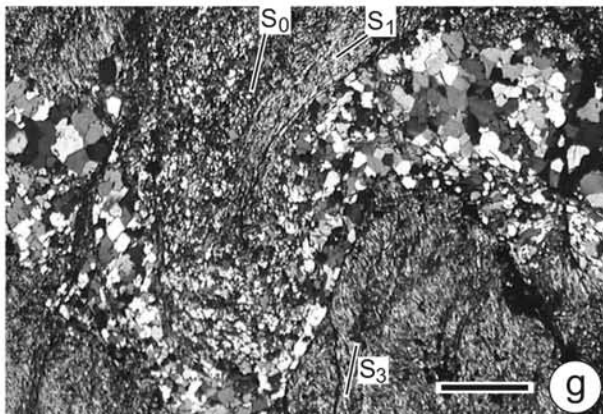
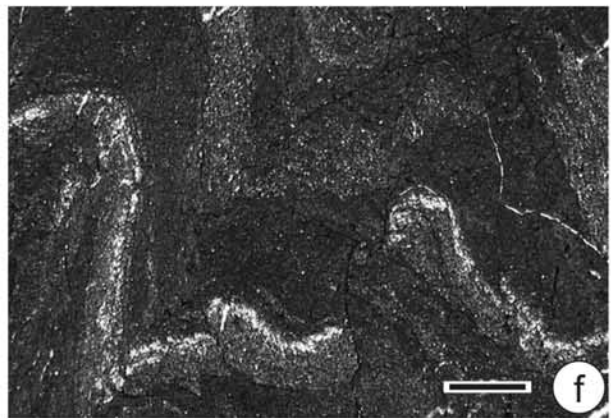
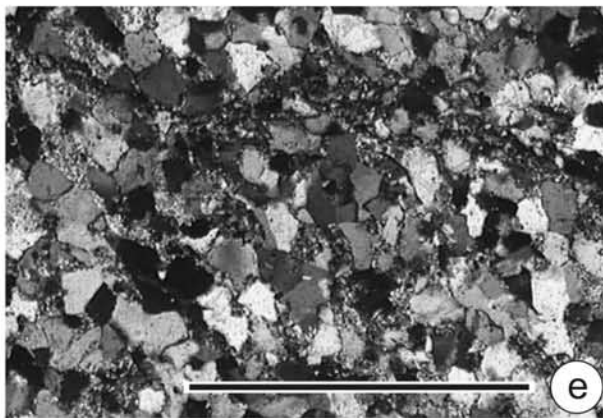
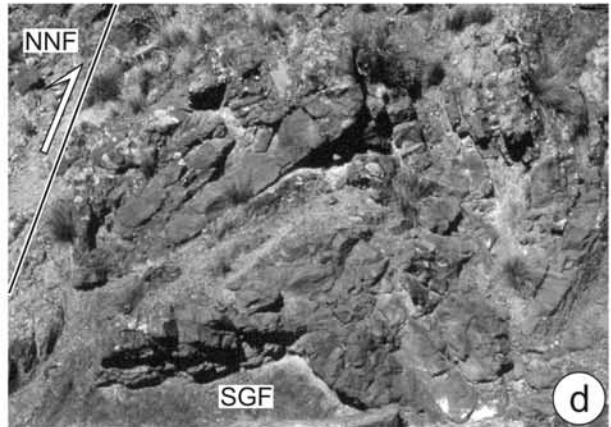
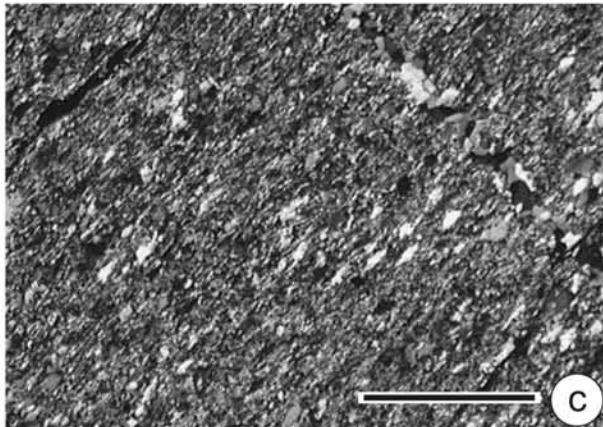
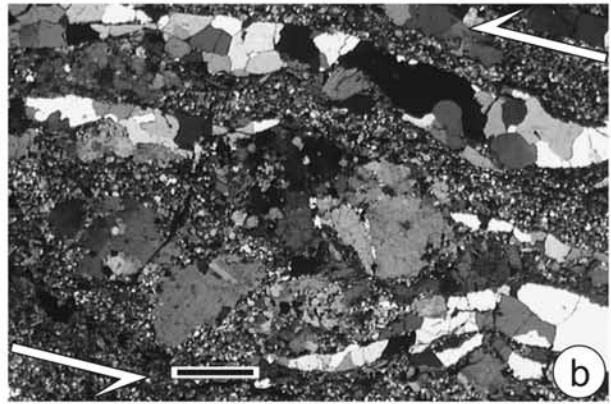
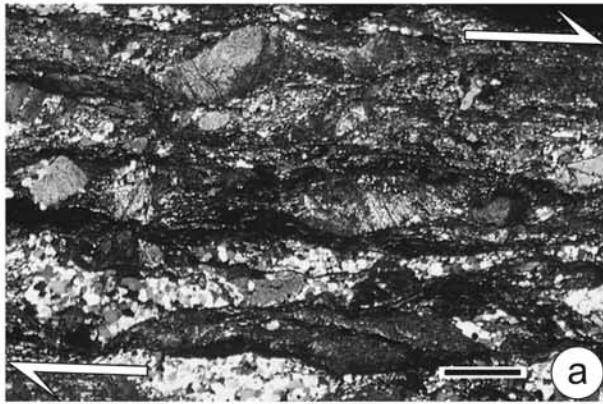
[37] Displacements at the base of the Nahuel Niyeu Thrust Sheet continued with the formation of shear planes and shear zones. These are parallel to or cut across the  $S_2$  foliation and partly also tight  $F_2$  folds. Single isolated clasts occur in the matrix of the foliated cataclasites. Kinematic indicators (S/C fabrics, shear bands, single asymmetric  $\sigma$ -shapes of quartz clasts) record a top-to-south directed sense

of shear and support the observations in the outcrops (Figure 5g). The growth of chlorite, epidote, and clinzoisite in syn- $S_2$  extension veins,  $S_2$  planes of the matrix, and foliated cataclasites also suggest conditions of a slight greenschist facies metamorphism probably at the boundary to the anchizone.  $C_3$  shear planes and shear zones, cutting across the main foliation mostly under great angles, are comparable with  $D_2$  structures in the Sierra Grande formation and are described below.

### 3.1.3.1.2. Contact Metamorphism Related to the Navarrete Granodiorite

[38] In the southern part of the Railer Thrust Sheet, contact metamorphism took place after formation of the penetrative  $S_2$  foliation.  $F_2$  folds are statically heated. Aside of muscovite, biotite is widely distributed in the foliated rocks. Quartz records static growth fabrics. Near the contact with the Navarrete granodiorite in the south, an additional static growth of porphyroblasts (? andalusites) took place across the penetrative and planar  $S_2$  foliation (straight internal fabrics). The porphyroblasts are entirely converted into sericite + muscovite  $\pm$  biotite  $\pm$  epidote aggregates.

[39] Only a few asymmetric  $\sigma$ -shapes of rotated porphyroblasts and pressure shadows support the model of final



emplacement-related movements of the pluton in the south which might have led to local shearing within distinct, incompetent layers of the schists. Such an interpretation is supported by observations from the unfoliated granodiorite at the contact. At the margins of some magmatic feldspar grains, small aggregates of feldspar recrystallization grains occur which do not follow a foliation or shear plane. Some feldspar grains are broken and crosscut by quartz-filled extension veins. In addition, magmatic quartz contains coarser subgrains and is recrystallized near zones of feldspar recrystallization. These features suggest that the solidified pluton margin has been affected by a slight compression under still elevated temperatures.

[40] Porphyroblast relics and heated  $D_2$  fabrics are overprinted by  $F_3$  crenulations,  $S_3$  cleavage planes, and  $C_3$  shear planes. The growth of sericite±muscovite + chlorite (at the expense of biotite) also in cleavage planes suggests a decrease in temperature after the final stage of contact metamorphism. At the intrusive contact, epidote±clinozoisite grew post- $D_2$  and syn- $D_3$  whilst quartz is deformed in the brittle-ductile transition. The  $D_4$  deformation led to bending, formation of crenulations and crenulation cleavage planes and was combined with the growth of sericite + chlorite±muscovite but without dynamic recrystallization of quartz.

### 3.1.3.2. Sierra Grande Formation

[41] The sandstones in the Rana Thrust Sheet are heterogeneously deformed. Beneath the Nahuel Niyeu Thrust they are slightly foliated parallel to bedding planes indicated by the growth of aligned sericite in the matrix and sericite±chlorite beards in pressure shadows. In other parts, tectonic compaction was accompanied by pressure solution at quartz-quartz contacts and sericite±chlorite growth between the clasts. In the matrix of foliated rocks, quartz is recrystal-

lized on a submicroscopical size. Quartz clasts are bent, kinked, and partly contain subgrains. Some of them record an overgrowth, separated from the core by a thin strip of opaque dust. Feldspar clasts are brittlely deformed.

[42] Within the thrust zone two successive stages of shearing could be directly compared with those within the basal phyllites of the thrust sheet above. The initial stage is marked by a penetrative  $S_1$  foliation parallel to bedding planes, indicated by aligned sericite and chlorite and dynamic quartz recrystallization in the matrix. Larger quartz clasts are bent, kinked, and partly replaced by subgrains plus recrystallization grains in high strain zones and at margins. All this suggests that metamorphic conditions were in the range of the slight greenschist facies during  $D_1$ .

[43] Continuing displacements led to the formation of shear zones and shear planes in the brittle-ductile transition with respect to quartz. The foliated cataclasites cut across the  $S_1$  foliation or are parallel and are comparable with those at the base of the Nahuel Niyeu Thrust Sheet (see above). Pieces of sheared and rotated clasts partly depict S/C fabrics with a top-to-south sense of shear (Figure 5h). Shearing was accompanied by the growth of sericite and dynamically generated quartz recrystallization grains on a submicroscopical size. Isolated fragments of coarse quartz clasts record bending, kinking, subgrain formation, and smallest-scale recrystallization grains within high-strain zones. Comparable fabrics were found in a thrust within the Sierra Grande formation.

[44] The second-stage cataclastic shear planes and shear zones are parallel to or cut across the sheared bedding under great angles. They are directly comparable with  $C_3$  shear planes and shear zones within the Nahuel Niyeu Thrust Sheet which are associated with open  $F_3$  folds and a developing  $S_3$  cleavage. Within the cataclasites only a diffuse foliation occurs. Quartz was deformed in the brittle-ductile transition. In wider shear zones, finest-grained

**Figure 12.** (opposite) Photomicrographs from thin sections, except (d). Scale bars are 1 mm long; crossed polarizers, except (f), with plane polarized light. (a) Mylonite of Tardugno type granodiorite (Yaminué Complex) depicting recrystallized quartz and asymmetric  $\sigma$ -shapes of feldspar porphyroclasts (top). Half arrows indicate the top-to-SW sense of shear (west of Nahuel Niyeu area, NW of Tardugno fault, ~0.7 km WSW of Puesto Tardugno). (b) Mylonite of Tardugno granodiorite with coarse recrystallization grains in elongated quartz layers. The  $\sigma$ -shape of broken feldspar porphyroclast indicates a top-to-SSW sense of shear (half arrows). The matrix consists of feldspar and quartz recrystallization grains (west of Arroyo Treneta, ~1.85 km NE of Puesto A. Curayá, road to Nahuel Niyeu). (c) Fine-grained and penetratively foliated mylonite of the Nahuel Niyeu formation at the base of the Sumuncura Thrust Sheet (Arroyo Salado area, east of Arroyo Salado, ~550 m SE of Puesto Alonso). (d) View toward east on steeply north dipping Sumuncura Thrust (left) along which phyllites of the Nahuel Niyeu formation (NNF) are carried southward over intensely folded sandstones of the Sierra Grande formation (SGF) in the footwall (outcrop is ~7 m long; central part of the W-E trending, southern segment of the Sumuncura Thrust in the Arroyo Salado area, ~1.25 km ESE of Puesto M. José). (e) Deformed sandstone of the Sierra Grande formation below the Sumuncura Thrust Sheet. Note slight deformation of quartz clasts and growth of aligned sericite in the matrix (Arroyo Salado area, north of Arroyo Salado, ~1.4 km NNE of Puesto M. José). (f) Open  $F_3$  folds in phyllite of the Nahuel Niyeu formation beneath the Sierra Grande formation. They are combined with  $S_3$  planes along which the limbs are partly sheared off and displaced (Arroyo Salado area, north of spot height 454, road to Puesto Alonso). (g) Open  $F_3$  folds in contact metamorphosed phyllite of the Nahuel Niyeu formation. Bedding ( $S_0$ ) is marked by layer of fine-grained quartz recrystallization grains and crosscut by  $S_1$  parallel quartz vein which consists of coarser recrystallization grains.  $S_3$  crenulation cleavage affects the muscovite-rich  $S_1$  planes (Arroyo Salado area, contact to the northern porphyritic granite SW of Puesto Alonso). (h) Sandstone of Sierra Grande formation from isolated occurrence north of Puesto Chico (north of the Arroyo Salado study area, compare map of Figure 18). The matrix consists of quartz recrystallization grains and new sericite. Note strain free recrystallization grains at the margins of quartz clasts.

quartz suggest that crystallization and recrystallization along with the growth of sericite±chlorite took place during and after shearing. The microfabrics show that this latest-stage shearing took place under T-conditions of the anchizone-greenschist facies transition. It was accompanied and outlasted by the growth of epidote/clinozoisite and chlorite.

### 3.1.3.3. Tardugno Granodiorite and Schists

[45] The proto-mylonites to mylonites of the Tardugno granodiorite record comparable microfabrics east and west of the Tardugno fault and in their equivalents of the Yaminué Complex. Their  $S_{my}$  foliation is depicted by aligned sericite, muscovite, chlorite, and ±biotite. Some relics of isoclinally folded quartz layers and crenulations within the foliation indicate a previous stage of deformation. In  $S_{my}$  planes flattened quartz is almost entirely replaced by recrystallization grains (Figure 12a). In many places their growth outlasted shearing under static conditions. Feldspar clasts are brittlely deformed, joints and fractures between broken and extended fragments and pressure shadows are filled with quartz and albite. Intracrystalline high-strain zones and sheared clast rims are covered by small, dynamically generated recrystallization grains which also occur in thin layers of the foliated matrix. New biotite is grown syn- to post- $S_{my}$  partly together with epidote/clinozoisite grains and grain aggregates. A younger local crenulation is related to mylonite formation because static annealing of quartz and the growth of sericite + muscovite + biotite outlast this event.

[46] These fabrics are comparable with those of the intensely foliated schists of the Yaminué Complex which consist of quartz + muscovite + biotite±feldspar±epidote/clinozoisite. In the foliation of the schists, relics of an older crenulated fabric could be detected. SW vergent intrafolial folds are associated with an axial-plane cleavage. In some parts, the cleavage planes turn into foliation-parallel, mica-rich layers which were used for shearing.

[47] The metamorphic conditions during mylonite formation were in the range of the greenschist facies. No indications for an amphibolite facies metamorphism were found. Statically annealed quartz (±feldspar) textures suggest a thermal input post- $S_{my}$  which can be related to a younger intrusive activity (Navarrete granitoids). A younger slight greenschist facies T-overprint is indicated by the growth of new epidote±clinozoisite along with chlorite, the latter mostly at the expense of biotite.

[48] The southwestern continuation of mylonites of the Tardugno granodiorite near Arroyo Treneta record microfabrics comparable to those in the Nahuel Niyeu area. Feldspar porphyroclasts are broken. Thin elongated quartz layers with some relics of isoclinal folds, however, consist of coarse recrystallization grains with straightened grain boundaries (Figure 12b). In the foliated matrix, feldspar and quartz are entirely recrystallized and form granoblastic textures. Biotite is recrystallized and randomly grew within pre-existing, biotite-rich layers. Subsequently, it was partly replaced by chlorite. The microfabrics show that high temperatures affected the rocks after cessation of mylonitization. This can be related to the intrusion of the Navarrete granodiorite and final emplacement of the Flores granite in this area.

[49] In the Tardugno granodiorite, asymmetric  $\sigma$ -shapes of pressure shadows at feldspar porphyroclasts (Figure 12a), quartz lenses, feldspar (Figure 12b), and feldspar bookshelf structures, single S/C fabrics and shear bands indicate a top-to-SW to SSW sense of shear parallel to the  $L_{my}$  lineation. In one location of the schists, an S/C fabric and the SW vergence of microfolds support this general sense of shear.

### 3.1.4. Interpretation of Thrusting and Subsequent Deformations

[50] The subsurface structures, depicted in the profiles of Figure 10, are interpretative. This also applies to the thicknesses of the units and the depths of the basal thrusts. The profiles show that the clastic sedimentary succession of the Sierra Grande formation in the subsurface extends further to the south. This interpretation is based on the imbricate of the Rana Thrust Sheet which is carried over phyllites of the Railer Thrust Sheet in the south. In the restored position, prior to thrusting, the sandstones of the Rana Thrust Sheet would represent the continuation of the clastic deposits in the subsurface. This implies that the phyllite succession of the Railer Thrust Sheet overthrust the Sierra Grande formation along a basal décollement (Railer Thrust). Thrusting must have taken place prior to the displacement of the Rana Thrust Sheet in the south and that of the Nahuel Niyeu Thrust Sheet in the north which caused the ramping of the Rana Thrust. This suggests that the phyllite succession of the Nahuel Niyeu formation in a wide area is thrust over the Sierra Grande formation. Hence, it is reasonable to assume that it represents a large thrust unit also outside this study area (see below).

[51] According to this picture, displacements of the Rana Thrust Sheet and Nahuel Niyeu Thrust Sheet belong to a second stage of thrust tectonics which, however, must not be separated by a long time gap. It is more reasonable to suggest that during a directly following stage of displacement the phyllite successions of the Nahuel Niyeu Thrust Sheet were cut out of the underlying phyllites along a ramp and then thrust over the Sierra Grande formation. A décollement operated within the basal parts of the Sierra Grande formation and permitted the ramping of the Rana Thrust Sheet in the south. Whether the Nahuel Niyeu Thrust represents the reactivated northern continuation of the initial Railer Thrust at the base of the Railer Thrust Sheet is unclear.

[52] In the Nahuel Niyeu and Sierra Grande formations all microfabrics show that thrusting took place under decreasing temperatures which is in accordance to the model of ramping thrust sheets. The  $D_1$  structures with clear sericite growth in the Rana Thrust Sheet (Sierra Grande formation) can be related to initial displacements of the Nahuel Niyeu Thrust Sheet. Both units were cut out of deeper crustal levels. The second-stage shear zone formation is related to the final displacements of the Nahuel Niyeu Thrust Sheet over the Sierra Grande formation in a higher crustal position.

[53] The general NE-SW trend of the Nahuel Niyeu Thrust does not indicate a general SE directed transport of the thrust sheet which was proposed by *Chernicoff and Caminos* [1996b] for their thrust slices. Kinematic indica-

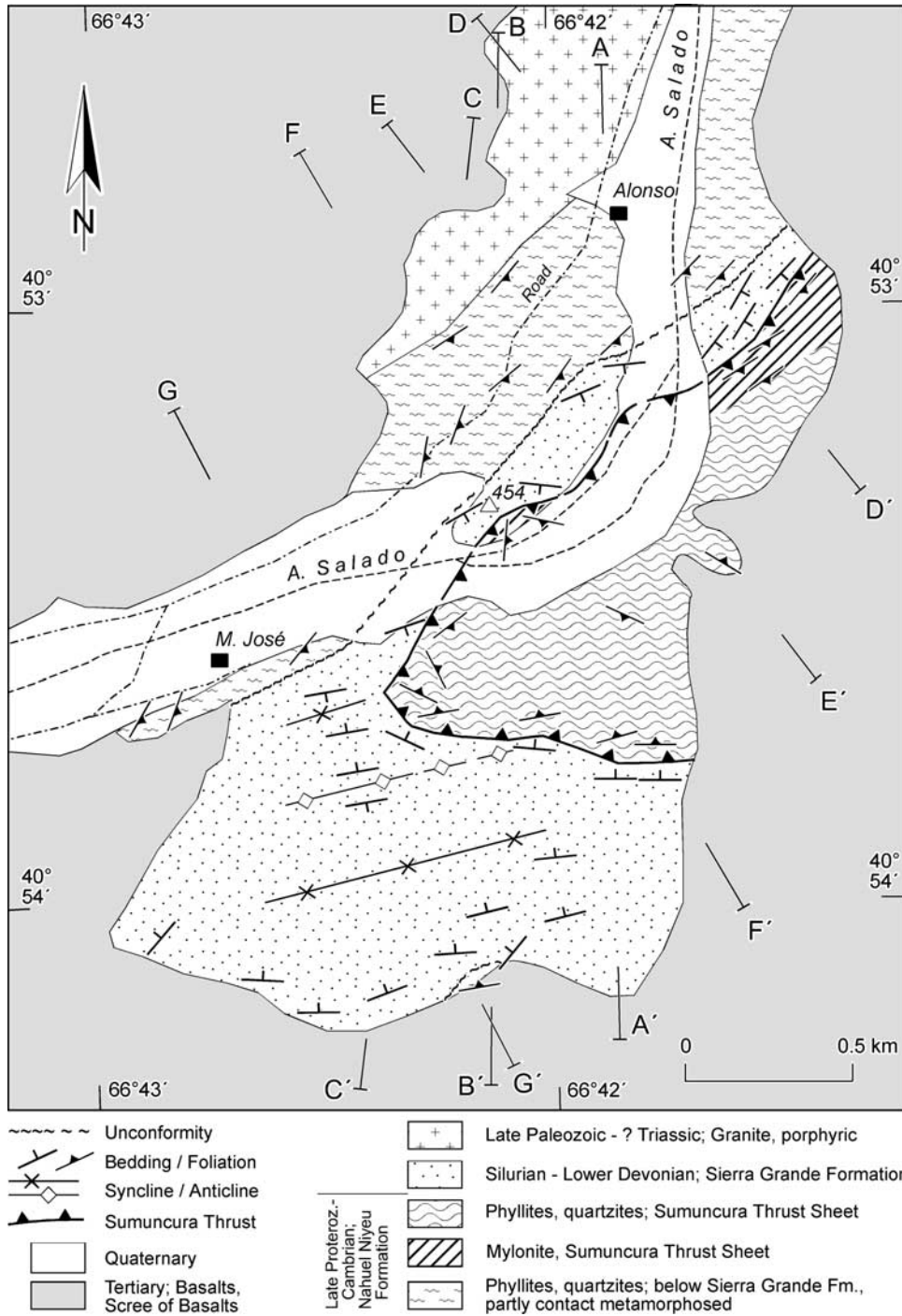


**Figure 13.** Geological sketch map of the study area in the southern part of Arroyo Salado, based on own field mapping (see Figure 2 for location). The lines of the profiles of Figure 14 are indicated.

tors and orientations of  $L_2$  lineations in the basal phyllites point to a ~S to SW directed transport which also applies to the Rana Thrust Sheet. The variable trend of strike of the Nahuel Niyeu Thrust and Rana Thrust can be explained by a combination of several factors. The approximately NE-SW trending parts could represent initial oblique to lateral ramps which were steepened, folded, and displaced along strike-

slip transfer faults during approximately NW-SE compression after cessation of thrusting (e.g., Nahuel Niyeu Thrust W of Arroyo Nahuel Niyeu). To a various extent the stacked units were folded around NE-SW trending axes and crosscut by younger reverse faults in the west (Figure 11).

[54] This deformation led to the formation of the Tardugno fault along which the foliated and mylonitized

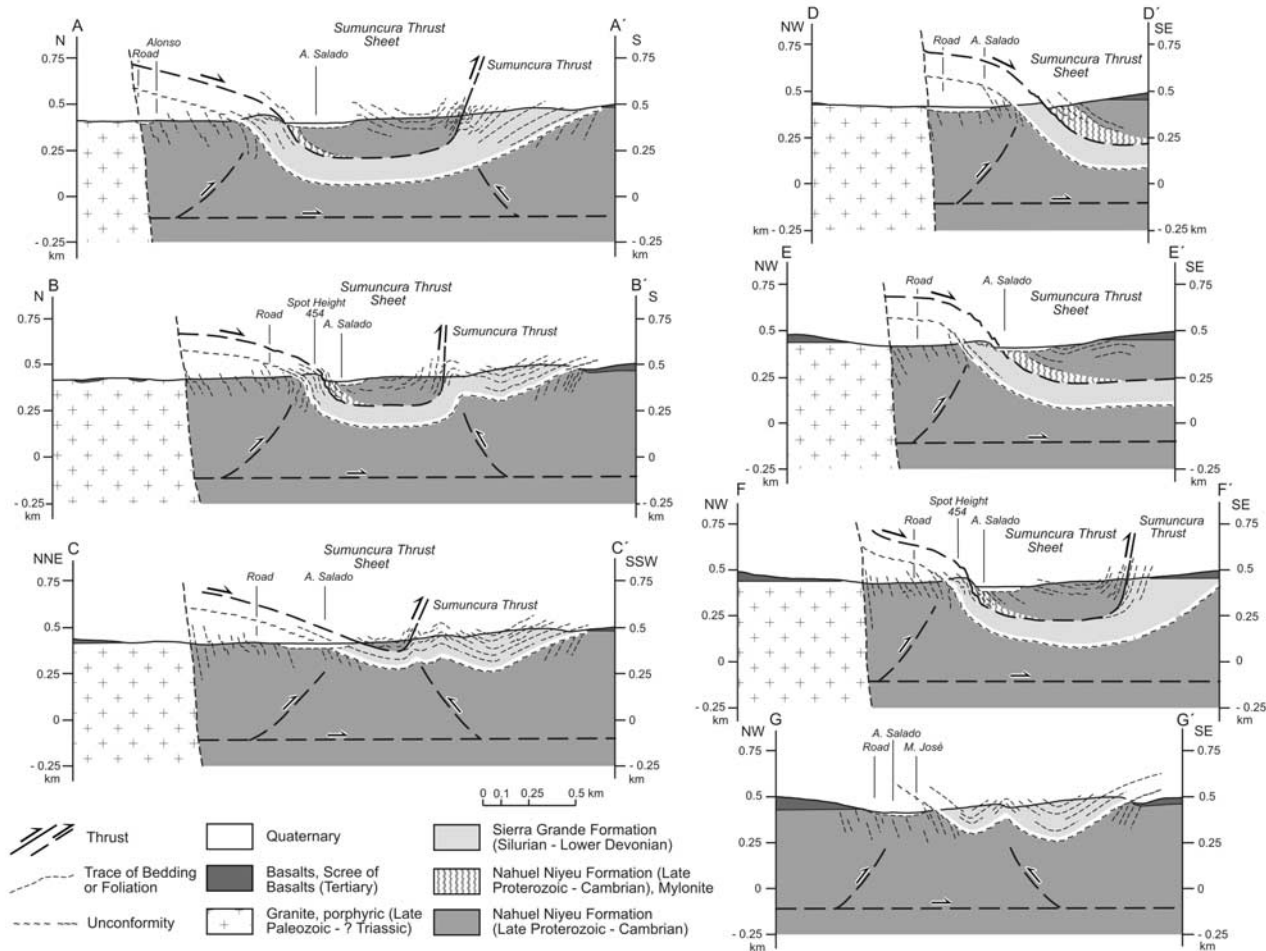


**Figure 14.** Geological profiles across the different units in the area of Arroyo Salado (for locations compare Figure 13).

Tardugno granodiorite and Yaminué Complex were uplifted (Figure 10; profile C–C'). Compression led to folding of the foliated granitoids with the formation of an  $F_2$  antiform northwest of the prominent fault. The granodiorite east of the fault is intruded by a granodiorite to granite assigned to the Navarrete Intrusive complex. As the age of this intrusion is unknown, and contacts also to the Nahuel Niyeu formation are not exposed, the mode of uplift of this part of the Tardugno granodiorite remains unclear.

[55] All this shows that the granitoids northwest of the fault line must have been located in a deeper crustal level which is supported by the microfabrics. Shear sense indicators demonstrate a SSW to SW directed transport of the hanging wall parallel to the lineation on the penetrative foliation or mylonite foliation. Comparable fabrics were detected within the deformed Tardugno granodiorite just west of Arroyo Treneta. Hence, it is probable that the foliated and mylonitized granitoids plus schists were part of an important ductile shear horizon in the subsurface and below the thrusts of the Arroyo Nahuel Niyeu area.

[56] This interpretation is more reasonable than a separation of the intense shear plus mylonitization as an older

event which is not supported by equivalents in the Nahuel Niyeu formation (e.g., older mylonites related to the  $D_1$  deformation). The above interpretation is furthermore supported by shear fabrics in the southern study area (see below) and different generations of younger fold structures which also overprint the phyllites of the Nahuel Niyeu formation with comparable geometries. Structures of these deformations under  $\sim$ NW-SE and  $\sim$ W-E compression were also found in the Navarrete granodiorite, whereas the Jurassic Flores granite is not deformed. This suggests that both plutons intruded the tectonically stacked units in the area of Arroyo Nahuel Niyeu and surroundings.

### 3.2. Southern Segment

[57] In the Arroyo Salado, about 32 kilometers SSW of the northern study area, a small area exposes phyllites of the Nahuel Niyeu formation and sandstone successions of the Sierra Grande formation (Figures 2 and 13) which have been briefly described by Cortés *et al.* [1984] and Caminos [1999]. In the north, a porphyric granite intruded the phyllites and is part of the Navarrete Intrusive Complex

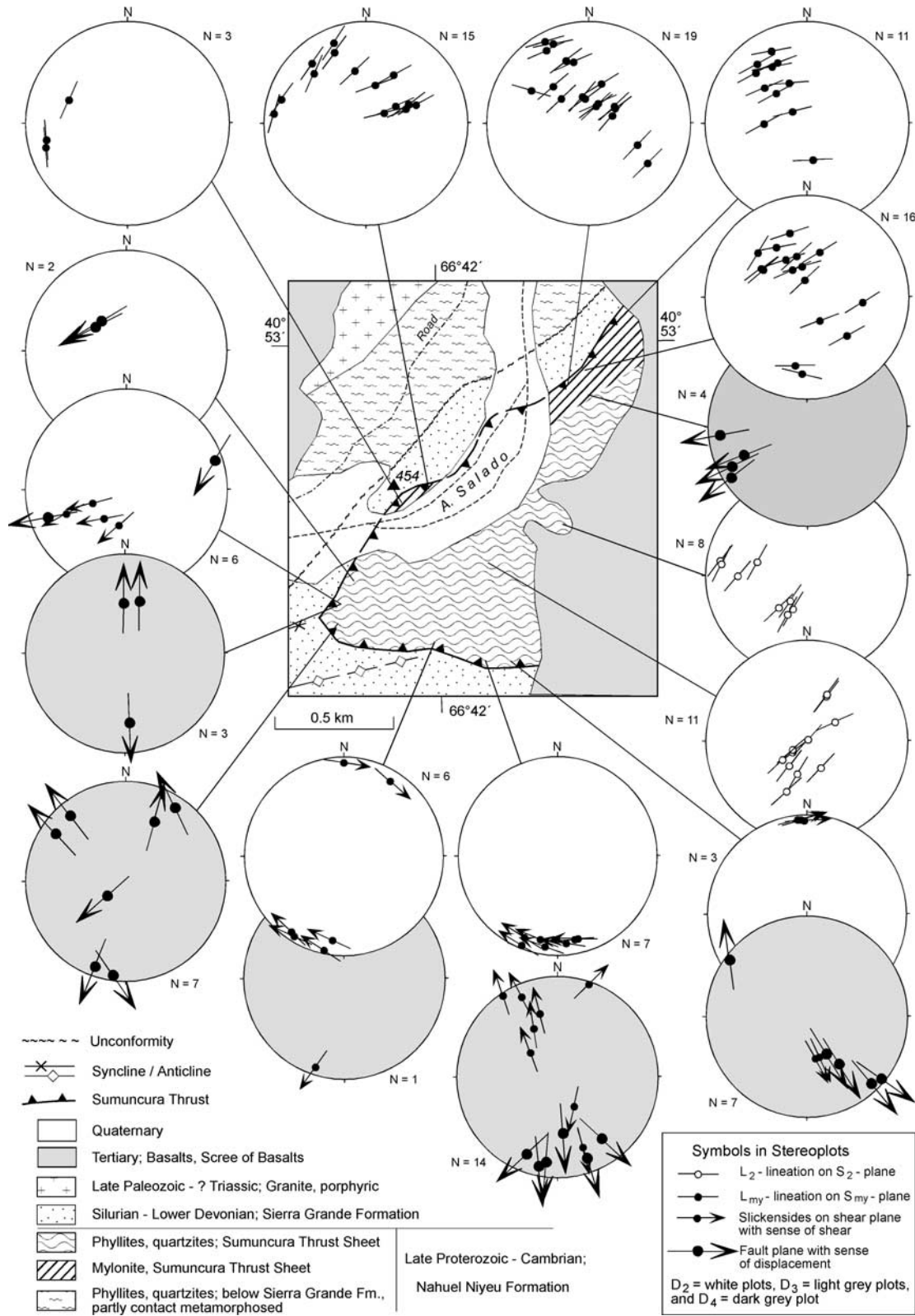


**Figure 15.** Lower hemisphere, equal-area stereograms of kinematic indicators in the Sumuncura Thrust Sheet (Arroyo Salado area), related to the locations on the map. In the Hoepfener plots [Hoepfener, 1955] the lineation is projected on the pole of the related plane, arrows indicate the relative sense of shear/displacement of the hanging wall units. White plots -  $D_2$  deformation; light grey plots -  $D_3$  deformation; dark grey plot -  $D_4$  deformation.

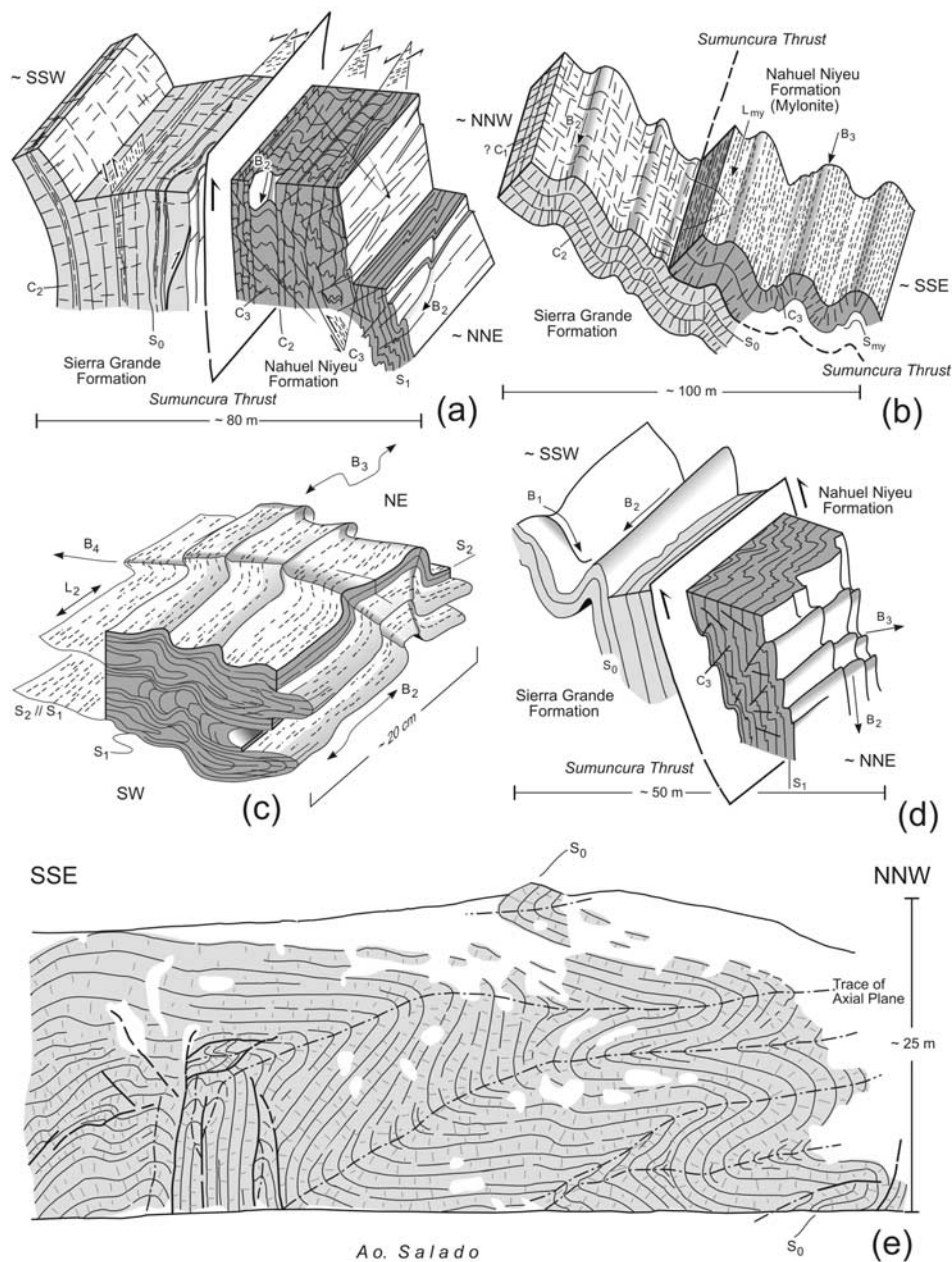


**Figure 16.** (a)–(d) Simplified, schematic, and composite block sketches of structures in the Arroyo Salado area. (a) and (d) show Sumuncura Thrust in its southern, approximately W-E striking segment. F<sub>2</sub> folds and related C<sub>2</sub> shear planes with sinistral displacements (a) are overprinted by south vergent F<sub>3</sub> folds (d) and conjugate sets of C<sub>3</sub> shear planes ((a) and (d) are located ~1 km and ~630 m ESE of Puesto M. José, respectively). (b) Sumuncura Thrust in its northern segment, east of Arroyo Salado (SE of Puesto Alonso). Along the penetrative foliation (S<sub>my</sub>) with a pronounced L<sub>my</sub> lineation, the mylonites overlie the bedding of the Sierra Grande formation in the footwall. Open F<sub>3</sub> folding in the mylonites with axes parallel to L<sub>my</sub> (F<sub>2</sub> in the Sierra Grande formation) also overprints the Sumuncura Thrust. (c) Detail from quartz-rich phyllites in the Sumuncura Thrust Sheet. Tight to isoclinal F<sub>2</sub> folds are combined with an axial-plane S<sub>2</sub> cleavage/foiliation which has a pronounced L<sub>2</sub> lineation. The older structures are overprinted by approximately SE vergent F<sub>3</sub> folds which in turn are bent around F<sub>4</sub> folds with different vergences (~1.24 km east of Puesto M. José). (e) Intense F<sub>2</sub> folding around ~NE-SW trending axes within sandstones of the Sierra Grande formation just west of Arroyo Salado (southeastern slope of ridge NE of spot height 454).

[Camino, 1999]. To the west, south, and east these units are covered by Tertiary basalts of the Meseta de Somuncura.

### 3.2.1. Sumuncura Thrust Sheet

#### 3.2.1.1. Macrofabrics

[58] Within the small area, the Sierra Grande formation is overthrust by phyllites of the Nahuel Niyeu formation. This thrust unit shall be named Sumuncura Thrust Sheet bounded by the Sumuncura Thrust at the base (Figure 13). On the map, the trace of the thrust depicts an oval trend, partly covered by Quaternary sediments of the Arroyo Salado.

[59] In the northern part, the phyllite succession of the Sumuncura Thrust Sheet lies with basal mylonites (quartz schists) on bedding planes ( $S_0$ ) of the Sierra Grande formation. The contact moderately to steeply dips toward approximately SE. The basal mylonites do not occur in the western, southern, and central part of the thrust sheet. Toward the south and at the base of the thrust sheet they seem to thin out above the Sumuncura Thrust (Figure 14). In the western part, intensely folded phyllites overlie SE to SSE dipping  $S_0$  planes of the Sierra Grande formation. In the southern part, the  $\sim$ W-E striking Sumuncura Thrust steeply dips toward  $\sim$ N or is vertical. On a general view, the Sumuncura Thrust Sheet represents a “half klippe” covered by Tertiary basalts of the Meseta in the east. Its spoon-shaped geometry is indicated by the different dip toward the center of the thrust sheet in the northern, western, and southern segments (compare Figures 13 and 14).

[60] The internal deformation of the Sumuncura Thrust Sheet can be separated into three stages as follows:

1. In the northern part thrusting took place parallel to the penetrative  $S_{my}$  foliation of the basal mylonites. A well-developed  $L_{my}$  lineation on the foliation is defined by elongated quartz and aligned sericite. It strikes approximately NE-SW (Figure 15). Macroscopic shear sense indicators could not be detected. In the western and southern part, approximately SW vergent  $F_2$  folds on a centimeter to decimeter scale can be replaced by isoclinal folds associated with an axial-plane  $S_2$  cleavage. Aside of the fold vergences, S/C fabrics and duplex structures indicate a transport of the thrust sheet toward approximately SW to WSW (Figure 16a). An  $L_2$  lineation on  $S_2$  cleavage planes and/or  $C_2$  shear planes strikes  $\sim$ NE-SW. This is comparable with the orientation of the  $L_{my}$  lineation within the mylonites (Figure 15).

2. In the northern part, the  $S_{my}$  foliation of the mylonites is bent around  $F_3$  folds whose NE-SW striking axes are parallel to the  $L_{my}$  lineation (Figure 16b). The open folds on a several meters and larger scale are symmetric or approximately NNW vergent. In the western and southern phyllites,  $F_3$  folds with NE-SW to W-E striking axes overprint the older structures (e.g.,  $F_2$  folds; Figure 16c). In the southern, W-E trending part of the Sumuncura Thrust,  $F_3$  folds are mostly approximately south vergent (Figure 16d). There, they are related to the final, southward directed and steep reverse displacement of the thrust sheet over the underlying sandstones of the Sierra Grande formation. The folds are combined with north and south dipping  $C_3$  shear

planes (Figures 16a and 16d). In the western and central parts of the thrust sheet, the folds also depict different vergences, can be replaced by kink bands, and are associated with  $C_3$  planes.

3. Within some parts of the Sumuncura Thrust Sheet the phyllites are bent around  $F_4$  folds with approximately N-S to NE-SW striking axes (Figure 16c). The folds on a decimeter scale are symmetric or record opposite vergences. They are accompanied by single shear planes.

#### 3.2.1.2. Microfabrics

[61] In the phyllites,  $S_1$  parallel sericite is bent around the hinges of flexural-slip  $F_2$  folds. Elongated quartz is bent, undulated, and records incipient formation of dynamically generated recrystallization grains. The  $S_2$  foliation is displayed by aligned sericite, chlorite, and  $\pm$ micro-biotite.

[62] The mylonite quartz schists consist of elongated quartz  $\pm$ plagioclase  $\pm$ k-feldspar clasts within a penetratively foliated matrix indicated by aligned sericite + chlorite  $\pm$ muscovite (Figure 12c). Dynamically generated, submicroscopical quartz recrystallization grains mostly occur at the margins of elongated quartz clasts and only in distinct parts fill the matrix. As in the phyllites they indicate that deformation took place under a slight greenschist facies metamorphism. Due to the small grain size and penetrative planar fabric, the sense of shear within the mylonites could not be clearly deduced in all thin sections. Single and clear asymmetric  $\sigma$ -shapes of quartz and feldspar clasts, developing S/C fabrics, and single shear bands demonstrate a top-to-SW sense of shear parallel to  $L_{my}$ .

[63] Sericite and  $\pm$ muscovite, aligned in the  $S_{my}$  foliation, are crenulated between developing  $S_3$  and  $C_3$  planes which are associated with open  $F_3$  fold structures. Some polygonal hinges show that sericite growth partly outlasted deformation. This is supported by newly grown sericite and dynamically generated quartz recrystallization grains on a submicroscopical size within  $S_3$  planes.

[64] In the phyllites to the south,  $S_3$  crenulation cleavage planes and  $C_3$  shear zones are displayed by aligned sericite and  $\pm$ chlorite together with angular fragments of quartz in shear zones.  $C_3$  shear planes are related to  $F_3$  flexural-slip and kink folds with disrupted and quartz-filled hinge zones and several extension veins on the limbs. Dynamic quartz recrystallization could not be detected. This shows that the  $D_3$  deformation in the phyllites presumably took place under anchizonal conditions, in contrast with the mylonites in the north.

### 3.2.2. Sierra Grande Formation

#### 3.2.2.1. Macrofabrics

[65] The Sumuncura Thrust Sheet is underlain by the Sierra Grande formation. Gliding of the thrust sheet took place parallel to bedding planes at the top of the sandstone succession. In addition, only single open bends around approximately N-S striking axes could be related to thrusting. In the southern part, however, the Sumuncura Thrust must have cut through the Sierra Grande formation along a ramp. This is indicated by the important thickness of the

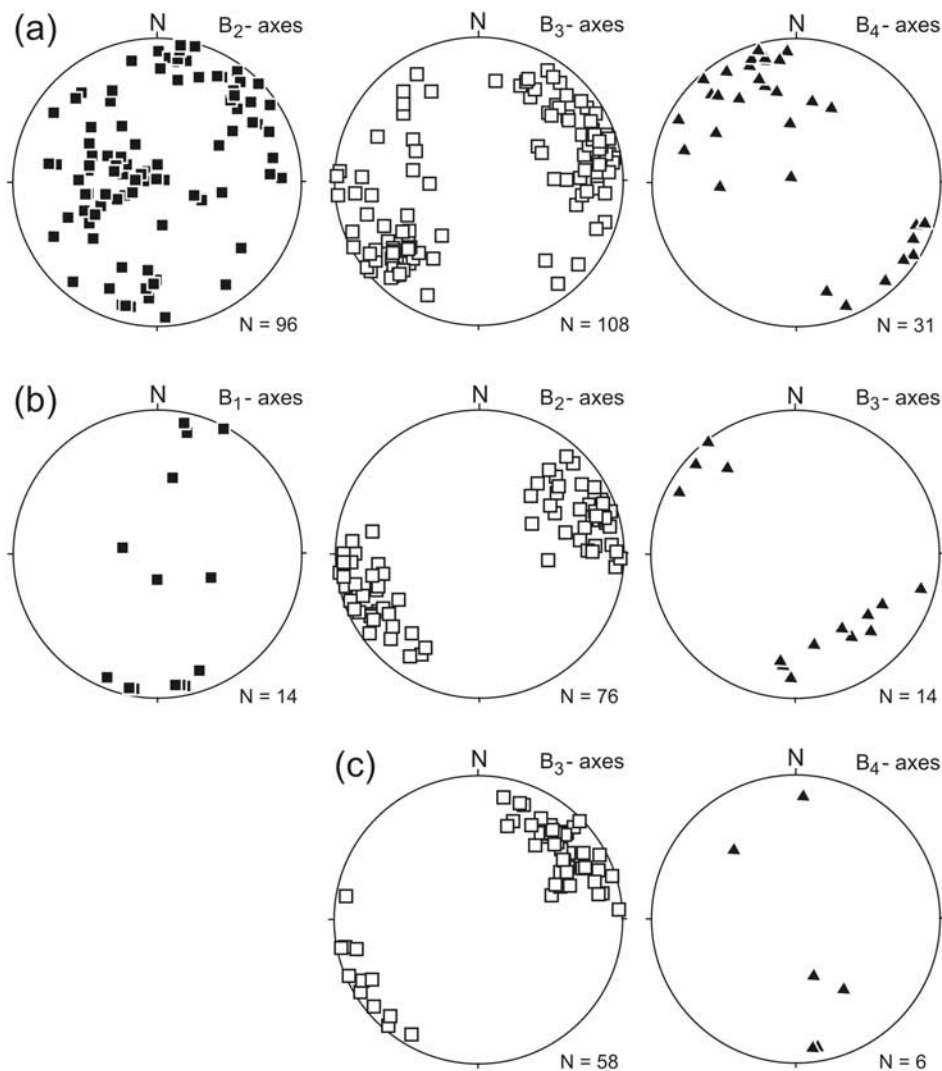


**Figure 17.** Lower hemisphere, equal-area stereograms of fold axes in the area of Arroyo Salado. (a) Sumuncura Thrust Sheet (Nahuel Niyeu formation). (b) Sierra Grande formation beneath Sumuncura Thrust Sheet. (c) Nahuel Niyeu formation beneath Sierra Grande formation (see text for further explanations).

Sierra Grande formation sandstones in the south compared with that in the northern and western parts (Figure 14).

[66] The steepening of the Sumuncura Thrust in the southern segment, combined with a final and local reverse displacement of the thrust sheet over the Sierra Grande formation, is related to the D<sub>2</sub> deformation of the sandstone succession. South of the thrust fault, it led to intense folding (Figure 12d) which passes into open synclines and anticlines around ENE-WSW striking axes further in the south (Figures 13, 14, and 17). The D<sub>2</sub> deformation can be compared with the D<sub>3</sub> event in the thrust sheet. In the western part of the Sierra Grande formation, single open F<sub>2</sub> folds with NE-SW striking axes occur. In the northern part, west of the Arroyo Salado, however, the sandstone succession beneath the thrust is intensely folded around NE-SW striking axes (Figure 16e). This F<sub>2</sub> folding is the equivalent of the F<sub>3</sub> folding of the mylonites at the base of the

Sumuncura Thrust Sheet and has also affected the Sumuncura Thrust (compare Figure 17).

[67] All this underlines that folding has affected the stacked units after cessation of thrust tectonics. It led to the steepening of the thrust fault in the north. The thrust probably has been bent around a large-scale, NE-SW trending anticline structure with a more shallowly dipping limb further northward (Figure 14). In the northern part of the Sierra Grande formation, just beneath the moderately to steeply approximately SE dipping Sumuncura Thrust, open F<sub>3</sub> folds on a several meters to tens of meters scale partly overprint older F<sub>2</sub> folds around ~N-S to NW-SE trending axes.

### 3.2.2.2. Microfabrics

[68] The sandstones were affected by tectonic compaction which led to pressure solution at quartz-mica and

quartz-quartz contacts and bending and kinking of clastic muscovite. Sericite grew between quartz clasts. In some parts, clastic quartz grains display overgrowths separated from the clastic core by opaque dust. In other layers, however, aligned sericite and sericite-chlorite beards at quartz clasts indicates a compaction with shear (Figure 12e). Finest-grained, dynamically generated quartz recrystallization grains occur in intra-crystalline high-strain zones of quartz grains. Sericite±chlorite beards at quartz clasts could be related only to this first stage of compression.

[69] Under different angles younger micro-shear planes and shear zones cut across the planes of compaction and shear. At and near the shear zones, ductilely deformed quartz contains finest-grained, dynamically generated recrystallization grains. In wider shear zones, angular relics of quartz clasts occur within the matrix. The latter consists of sericite and submicroscopical quartz grains which partly may represent recrystallization grains. Shearing also led to brittle fracturing of quartz. The shear zones pass into brecciated parts with diffuse boundaries and without clear preferred orientation. Taken together, these observations show that after the first shear event under slight greenschist facies metamorphism the formation of younger shear zones began in the brittle-ductile transition and continued under brittle conditions with the formation of breccias. These stages can be compared with those in the Sierra Grande formation of the Arroyo Nahuel Niyeu in the north.

### 3.2.3. Nahuel Niyeu Formation Below the Sierra Grande Formation

#### 3.2.3.1. Macrofabrics

[70] Along a basal angular unconformity, the Sierra Grande formation overlies the phyllites of the Nahuel Niyeu formation [Cortés *et al.*, 1984; Caminos, 1999] (present Figures 13 and 14). In the northern part, the unconformity is exposed in several outcrops and dips toward approximately SE. In the western part, a dip toward SE could be inferred. In the south, the north dipping angular unconformity could be fixed in a small occurrence of phyllites below the sandstone succession north of the cover of Tertiary basalts scree.

[71] Beneath the unconformity,  $S_1$  foliation planes of the phyllites of the Nahuel Niyeu formation steeply dip toward approximately SE (western and northern part) or approximately NW (southern part). Within the phyllites no clear crosscutting relationships between bedding planes and  $S_1$  foliation planes could be detected. Equivalents of the widely distributed  $D_2$  structures within the Sumuncura Thrust Sheet could not be found. Single NW vergent  $F_3$  folds around approximately NE-SE striking axes, mostly on a centimeter to decimeter scale, are considered equivalent to the  $F_2$  folds of the Sierra Grande formation (Figure 17). They indicate the approximate NW-SE compression of the Sierra Grande formation plus stacked Sumuncura Thrust Sheet. The final compressive deformation, documented in all the other units by open fold structures with approximately N-S to NW-SE striking axes, is recorded by  $F_4$  folds on a centimeter to decimeter scale also within the basal phyllites.

[72] The steeply ~SE dipping phyllites of the Nahuel Niyeu formation were intruded and contact metamorphosed by the porphyric granite in the north (Figures 13 and 14). The intrusive contact follows the trend of the  $S_1$  foliation in the country rocks. Contact metamorphism affected all structures of the phyllites comprising also  $F_3$  folds with approximately NE-SW striking axes. Only younger, ~NNE-SSW to NE-SW striking and subvertical dextral shear planes cut across the granite and contact metamorphosed phyllites.

#### 3.2.3.2. Microfabrics

[73] In fine-grained phyllites, south of the granite intrusion,  $S_1$  planes are crenulated between  $S_3$  cleavage planes where sericite is realigned. The cleavage planes are associated with  $F_3$  flexural-slip to kink folds whose hinges zones are partly sheared off (Figure 12f). Fold hinges and limbs are dissected by quartz-filled extension veins, joints, and fracture planes. Ductile deformation and incipient recrystallization of quartz and the growth of chlorite (±micro-biotite) syn- to post- $S_3$  suggest a metamorphic overprint in the greenschist facies-anchizone transition.

[74] At the southern intrusive contact of the porphyric granite,  $F_3$  fold structures in the contact metamorphosed phyllites can directly be compared with those in the south (Figure 12g). The folds are combined with crenulations of the  $S_1$  foliation which are associated with  $S_3$  crenulation cleavage planes. The size of phyllosilicates at the contact is enlarged. Muscovite is aligned parallel to  $S_1$  and displays polygonal textures in crenulations suggesting growth and/or recrystallization of muscovite syn- to post- $F_3$ . Thus, bent muscovite occurs aside of polygonally recrystallized muscovite within the same crenulation. Realigned and new muscovite display the  $S_3$  planes. Furthermore, muscovite and chlorite randomly grew across crenulated  $S_1$  planes. Recrystallization and static grain growth of quartz with the formation of triple junctions also indicate that heating outlasted  $D_3$  under static conditions.

[75] These observations show that  $F_3$  folding and associated  $S_3$  cleavage formation interfered with heat transfer from the granite pluton. The latter may have started some time during the  $F_3$  event (growth with increasing grain size of muscovite) and outlasted deformation under static conditions (grain growth of quartz, polygonal muscovite textures in  $F_3$  crenulations). Hence, it is concluded that the porphyric granite is a late synkinematic intrusion with respect to the  $D_3$  event. This is also based on the fact that the granite margin does not show evidence for the  $D_3$  deformation in the outcrops.

#### 3.2.4. Interpretation of Thrust Tectonics

[76] Thrusting of the Sumuncura Thrust Sheet took place toward approximately SW over the flat-lying Sierra Grande formation. Gliding along the Sumuncura Thrust used the bedding planes in the underlying sandstones. Only in the south, the thrust cuts across the Sierra Grande formation along a ramp. The mylonites at the base of the thrust sheet indicate a long-distance transport of the Sumuncura Thrust Sheet from deeper crustal levels upward under ductile

deformation of quartz. During continuing displacement along the basal thrust they must have been partly cut off (compare Figure 14), and deformation continued under conditions within the brittle-ductile transition.

[77] After stacking of the Sumuncura Thrust Sheet, approximately NW-SE compression led to folding around mostly ~NE-SW striking axes affecting the thrust sheet, Sumuncura Thrust, and underlying units (Figure 17). The phyllites at the ramp in the south were steepened and reverse faulted over the underlying sandstones, combined with folding in the footwall. In the north, the stacked units were bent around a large-scale, approximately NE-SW striking antiform structure and in part intensely folded.

[78] The microfabrics suggest that the top of the Sierra Grande formation, just beneath the Sumuncura Thrust, has been affected by heterogeneous deformation. Adjacent rocks either record tectonic compaction or are sheared. This supports the field observations that more intense shearing and internal deformation at and near the thrust are restricted to thin layers. This also applies to the internal deformation of the Sierra Grande formation in general: shearing and/or bedding-parallel slip took place within thin and distinct layers. The first-stage shearing is attributed to the emplacement of the Sumuncura Thrust Sheet whereas the second stage in the brittle-ductile transition with respect to quartz is related to final displacements of the thrust sheet. Thus, the deformational history can be compared with that in the Nahuel Niyeu area.

[79] Folding of the stacked units after cessation of thrusting and bending of the Sumuncura Thrust are explained here to have been accommodated by an active décollement in the subsurface (Figure 14). As the Sierra Grande formation overlies the phyllites of the Nahuel Niyeu formation along an angular unconformity, the décollement must be placed within the phyllites of the footwall. Its depth and areal extent are unclear (see below). In addition, ~NW and ~SE dipping reverse faults, branching off the subsurface décollement, might have accommodated shortening during this stage of compression. There was no evidence found, however, that such branching faults cut across the stacked units and reached the surface. Hence, it is assumed that they ended blind within the folded Nahuel Niyeu formation.

[80] The porphyric granite in the northern part of this study area intruded the tectonically stacked and subsequently folded units and heated the phyllites of the Nahuel Niyeu formation. In view of the geological map and profile reconstructions (Figures 13 and 14), it is probable that the intrusion followed the trend of the  $S_1$  planes in the phyllites and also that of the large-scale (eroded), NE-SW trending antiform which was formed after cessation of thrusting. Final compression locally affected the folded stack of units by folding around approximately N-S to NW-SE striking axes. The effects of this deformation on the porphyric granite are unclear.

#### 4. Age of Deformations and Intrusions

[81] The Nahuel Niyeu Thrust Sheet and Railer Thrust Sheet were intruded by the Navarrete granodiorite to granite

(Figures 3 and 10). Within the pluton, structures related to thrust faulting could not be detected (e.g., ductile foliation planes and/or ductile shear planes). Hence, the pluton must be younger than thrust tectonics [see also *Chernicoff and Caminos*, 1996b].

[82] Results of radiometric dating from the Navarrete Intrusive Complex are not conclusive. The data scatter from Carboniferous to Triassic ages which might be related to the effects of Jurassic intrusive activity [cf. *Pankhurst et al.*, 1993]. A previously published Carboniferous age of the Navarrete Granite [*Caminos et al.*, 1988] is regarded as no longer valid, and a correlation of the most voluminous granites of the Somuncura Batholith with the Permo-Triassic Choiyoi province is proposed [*Pankhurst et al.*, 1992]. As it is unlikely that the deposition of the Sierra Grande formation was terminated during the Lower Devonian, and Triassic volcanics are not affected by compressive deformation, a Late Paleozoic (probably Permian) age for thrust tectonics seems to be reasonable.

[83] The following deformation under approximately NW-SE compression affected the Navarrete granodiorite. The evidence is shown by several observations: (1) folding of the contact metamorphosed phyllites within the Railer Thrust Sheet north of the intrusive contact; this was combined with a NNE-SSW striking sinistral strike-slip fault which displaces the intrusive contact; (2) clasts of the granodiorite to granite occur within the breccia to cataclasite of the Tardugno fault; (3) shear planes of this overprint cut across the intrusion. Based on the imprecisely defined age of the Navarrete granodiorite, a Permian age for this deformation can be assumed. If one accepts, however, that the late synkinematic intrusion of the porphyric granite in the Arroyo Salado area represents the latest stage of the Navarrete Intrusive Complex [*Caminos*, 1999] then a Permo-Triassic age of its emplacement and also the final stage of approximately W-E compression is possible.

[84] One Rb-Sr date point to a Precambrian age of the Tardugno granodiorite [*Caminos et al.*, 1994]. The granodiorite is ductilely deformed and subsequently intruded by the Navarrete granodiorite to granite. It is reasonable to suggest that the Tardugno granodiorite intruded the psammopelitic sediments of the Yaminué Complex which may represent equivalents of the Late Proterozoic to Cambrian Nahuel Niyeu formation. Relics of tight to isoclinal microfolds within the mylonite foliation of both rock types indicate the existence of one older deformational event which can be compared with (? Cambrian)  $D_1$  structures in the Nahuel Niyeu formation.

[85] The heterogeneous foliation and mylonitization under greenschist facies metamorphic conditions are attributed here to Late Paleozoic thrust tectonics. Microcrenulations with axes parallel to  $L_{my}$  are interpreted as the effect of continuous shearing and are considered equivalent to structures of the  $D_2'$  deformation at the base of the Nahuel Niyeu Thrust Sheet. However, based on the Tardugno fault in the east, having uplifted the northwestern block with respect to the phyllites of the Nahuel Niyeu Thrust Sheet, the mylonites must have been formed within a deeper crustal ductile shear horizon. Thus the effects of a higher temperature

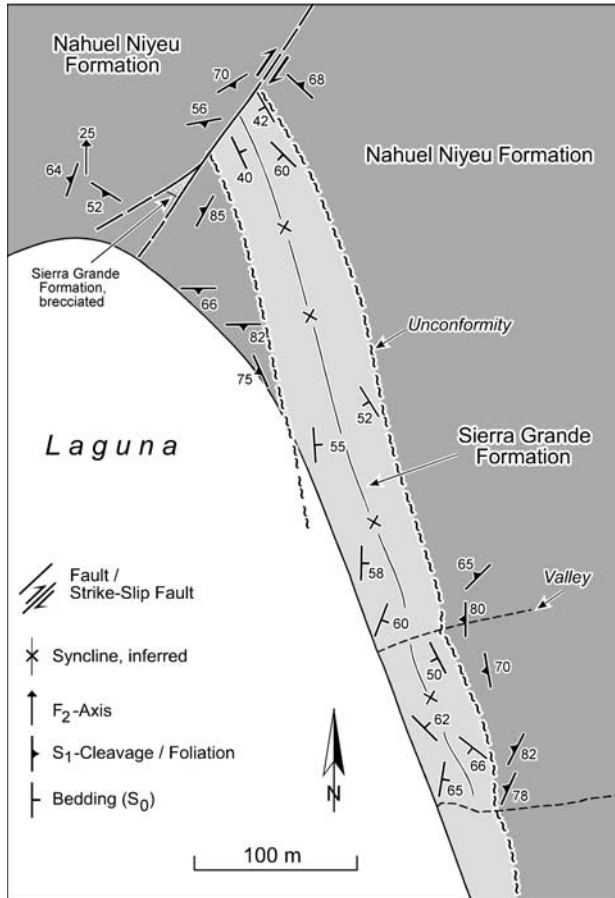


**Figure 18.** Geological sketch map of the small occurrence of sandstones of the Sierra Grande formation west of Arroyo Salado near Puesto Chico, based on field mapping (for location compare Figure 2).

overprint do not account for a greater age of mylonite formation plus metamorphism (e.g., Early Paleozoic).

### 5. Synthesis and Interpretation

[86] Thrust tectonics in both study areas, separated from each other over a distance of more than 30 km, show that compressive deformation with crustal shortening was not only a local phenomenon. On the contrary, it is probable that thrust tectonics in the northeastern part of the North Patagonian Massif was widely distributed. This is indicated by the directly comparable deformational history in both study areas. Thus the structures only depict cutouts of a large fold-and-thrust belt which is widely covered and obscured by younger volcanic rocks and plutons, respectively.

[87] A small occurrence of the Sierra Grande formation in the northern part of the Arroyo Salado near Puesto Chico, approximately 17 km north of the southern study area (Figures 3 and 18), gave an additional insight. There, the sandstones overlie phyllites of the Nahuel Niyeu formation without evidence for a tectonic contact at the base. They are

bent around an open, NNW-SSE striking syncline structure and are cut off along a dextral strike-slip fault in the north.

[88] On a microscale, the sandstones record widely distributed quartz recrystallization between quartz clasts (Figure 12h). Boundaries of recrystallization grains are straight to slightly curved. They indicate a thermal overprint which outlasted tectonic compaction under static conditions. It can be attributed to the thermal effects of an intrusion. Compaction is recorded by sericite growth between quartz clasts with a partly preferred orientation. However, ductile cleavage planes or shear planes could not be detected. It is assumed that this occurrence represents the northern continuation of the Sierra Grande formation in the south with a basal sedimentary contact (Figure 19). This would imply that the sandstones were overthrust by the Sumuncura Thrust Sheet or an equivalent.

[89] It is reasonable to assume that both areas with thrust tectonics are connected with at least one basal décollement in the subsurface (“Floor Thrust”; Figure 19) which was active during the second stage of compression. It is unclear, however, whether the Sumuncura Thrust Sheet represents the southern equivalent (? or continuation) of the Railer Thrust Sheet in the north. Both consist of phyllitic rocks of the Nahuel Niyeu formation which tectonically superpose the Sierra Grande formation. This indicates that great portions of the Sierra Grande formation either are hidden in the subsurface or were lifted and eroded during subsequent folding. Hence, the shallow marine sediments probably have (had) a wide areal distribution in this part of the North Patagonian Massif. This interpretative picture, however, does not exclude the possibility that additional thrust faults or imbricates exist in the line of the transect of Figure 19. Based on the reconstruction, displacements along the thrusts can conservatively be estimated to have been in the range of a few kilometers. If a connection between both thrust sheets in the northern and southern areas will turn out to be true, this would drastically increase the amount of displacements.

[90] The inferred Floor Thrust is shown to be connected with the Tardugno fault along which mylonites of the Tardugno granodiorite and the Yaminué Complex were uplifted. It is suggested that the ductilely deformed rocks were cut out of a ductile shear horizon in the subsurface. The depth of this horizon, as those of the other thrusts in the subsurface, is unclear and only schematically depicted in Figure 19.

[91] A few observations from poorly exposed relics of the Sierra Grande formation southeast and east of the village of Nahuel Niyeu (Figure 2) suggest that they record a steep dip of bedding planes. Exposed contacts to the phyllites could not be found. Hence, it is unclear whether these occurrences lie above the succession of phyllites (e.g., on top of the Nahuel Niyeu Thrust Sheet) or are (partly) involved into thrust tectonics. Microfabrics in the sandstones from the Ruta Nacional 23 east of Arroyo Nahuel Niyeu are entirely different to those in the Rana Thrust Sheet. In particular, no indications for tectonic compaction, shearing, cleavage planes, and sericite growth were found. This suggests that this part of the Sierra Grande formation lies in an uppermost

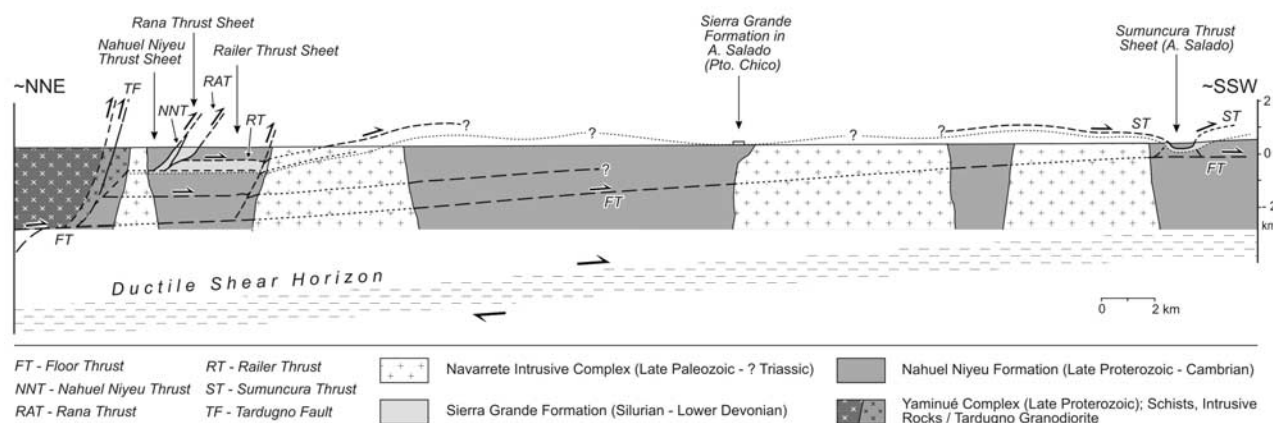


**Figure 19.** Interpretative profile across the different tectonic units between Nahuel Niyeu and the southern part of Arroyo Salado. Depths of décollements in the subsurface are inferred. The existence and position of a schematically depicted ductile shear horizon are assumed. Inferred continuations of thrusts and lithological units across the plutons of the Navarrete Intrusive Complex only depict the correlation and do not necessarily imply displacements of the igneous bodies (see text for further explanations).

tectonic position on top of the Nahuel Niyeu Thrust Sheet and in sedimentary contact with the phyllites. Therefore, it cannot be compared with the tectonic position of equivalent rocks in the Rana Thrust Sheet.

[92] The Navarrete granodiorite has intruded the tectonically stacked units and was affected by the following, ~NW-SE compression. The porphyric granite in the Arroyo Salado area, however, was late-synkinematic with respect to this event. This shows that different plutons were generated during the deformational history. It is noteworthy that granitoids in this part of the North Patagonian Massif often display an approximately NE-SW to NNE-SSW trend on the map (Figure 2). They appear to follow the trend of the folding around ~NE-SW striking axes which took place after cessation of thrust tectonics.

## 6. Implications for a Patagonia Plate

[93] In view of the configuration of different crustal blocks north of extra-Andean Patagonia (Figures 1 and 20), it is obvious that the Early Paleozoic Cuyania (Pre-cordillera) Terrane can be traced from central western Argentina via the San Rafael Block up to the Las Matras Block in the southeast [Melchor *et al.*, 1999; Sato *et al.*, 2000]. The southern continuation of the belt of metamorphic units in the east, deformed and metamorphosed during the Early Paleozoic Famatinian orogeny, can be seen in the Chadileuvú Block of the La Pampa Province north of Patagonia where also undeformed granitoids occur [Tickyj *et al.*, 1999a, 1999b; Sato *et al.*, 2000] (present Figure 20).

[94] Within the studied northeastern segment of the North Patagonian Massif no clear evidence for a southern or southeastern continuation of this belt of Famatinian deformation has been found up to now. This is supported by Ordovician granitoids of the Punta Sierra formation, dated by Varela *et al.* [1997, 1998], which intruded the simply deformed (D<sub>1</sub>) and metamorphosed phyllite succession of

the El Jagüelito formation (equivalent of the Nahuel Niyeu formation). The granitoids were not ductilely deformed. After a period of uplift and erosion they were unconformably overlain by the sandstone succession of the Silurian to Lower Devonian Sierra Grande formation. It is important to note that the deposition of clastic successions in the Sierras Australes north of Patagonia has been attributed to the Ordovician to Permian time interval [Buggisch, 1987; von Gosen and Buggisch, 1988]. Hence, there seems to be a difference in the evolution during the Ordovician which is indicated by granitoid intrusions in northeast Patagonia. Structures of compressive deformation found are younger than the Sierra Grande formation. During post-Lower Devonian time, however, Famatinian deformation and metamorphism in central western Argentina were still terminated.

[95] For the northeastern segment of the North Patagonian Massif, compressive deformation in two other areas support the picture from the above study areas west of Valcheta:

1. Mylonites of the Peñas Blancas granite and La Laguna granite west of Mina Gonzalito (Figure 20), discovered by Giacosa [1996], record an approximately SW or NE directed sense of shear [Giacosa, 2001; von Gosen, 2002]. The Peñas Blancas granite is interpreted as part of the Permian Pailmán granite [Giacosa, 1997], whereas the age of the La Laguna granite is unclear. The La Laguna granite has been affected by shearing and mylonitization of the Peñas Blancas granite and subsequently was intruded by the La Verde granite. This situation can be compared with the intrusion of the Navarrete granodiorite into the foliated Tardugno granodiorite.

2. Ductile deformation in this part of the North Patagonian Massif can be related to the above thrusting in the area of Nahuel Niyeu-Arroyo Salado. The important thickness of the La Laguna granite (mylonite) as well as the widely foliated to mylonitized intrusion in the Nahuel Niyeu

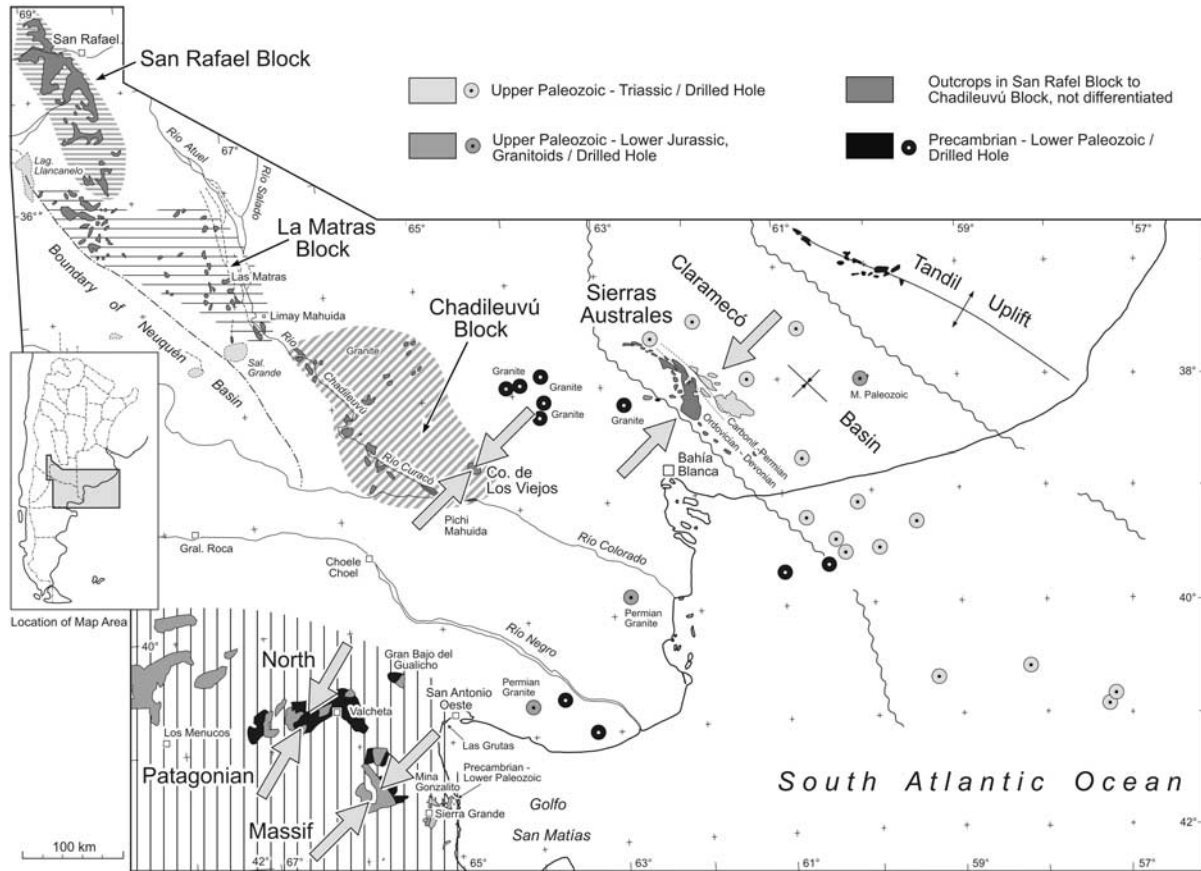


**Figure 20.** Simplified map of the main tectonic units in the area between the North Patagonian Massif, Sierras Australes, and San Rafael Block. Thick gray, double arrows indicate the broadly estimated orientations of compression in the northeastern segment of the North Patagonian Massif (this study and area west of Mina Gonzalito), Co. de Los Viejos (La Pampa Province), and Sierras Australes (Buenos Aires Province), based on the literature cited in the text. Map compiled and adapted after *Criado Roque and Ibáñez* [1979], *Linares et al.* [1980], *Rossi and Zanettini* [1986], *Tickyj and Llambías* [1994], *Fryklund et al.* [1996], *Tickyj et al.* [1997], *Caminos and Espejo* [1999], *Cingolani and Varela* [1999], *Melchor et al.* [1999], and *Sato et al.* [1999, 2000].

area support the interpretation of (an) important ductile shear horizon(s) generated during initial thrust tectonics.

3. In the area of Sierra Grande up to the Atlantic coast (Figure 20), the Sierra Grande formation is folded around open synclines and anticlines with a variable approximately N-S trend of the axes. Folding is accompanied by reverse faults and partly strike-slip faults. South of Sierra Grande, cooling of the Laguna Medina granite and granodiorite interfered with the deformation of the intruded Sierra Grande formation and is interpreted as of Permian age [Rossello et al., 1997; von Gosen, 2002]. A late Early to Late Permian age of deformation is indicated by paleomagnetic studies of Rapalini [1996, 1998]. Deformation under approximately NW-SE to approximately W-E compression in this sector of the North Patagonian Massif can be compared with the deformations after cessation of thrust tectonics in the areas of Nahuel Niyeu and Arroyo Salado.

[96] The deformational structures found in the above study areas of this segment of the North Patagonian Massif

record three successive stages of compression which permit to broadly estimate the orientation of the maximum compressive stress component ( $\sigma_1$ ). It changed from the approximately NE-SW orientation (stage 1) counter-clockwise over approximately NW-SE (stage 2) into an approximately W-E trend (stage 3). Stage 1 can be related to collision tectonics, whereas both subsequent stages could indicate post-collisional compression.

[97] North of the North Patagonian Massif, an approximately NW-SE striking granite mylonite has been described from the Cerro de los Viejos in the La Pampa Province by Tickyj and Llambías [1994] and Tickyj et al. [1997, 1999a] (present Figure 20). They report an approximately NE-SW compression with a relative sense of shear of the southwestern hanging wall toward NE. The deformation has been interpreted as the result of a NE directed push (or collision) of Patagonia [Tickyj et al., 1997] and attributed to the Carboniferous-Permian boundary [Tickyj et al., 1999a]. It can be compared with the above mylonite

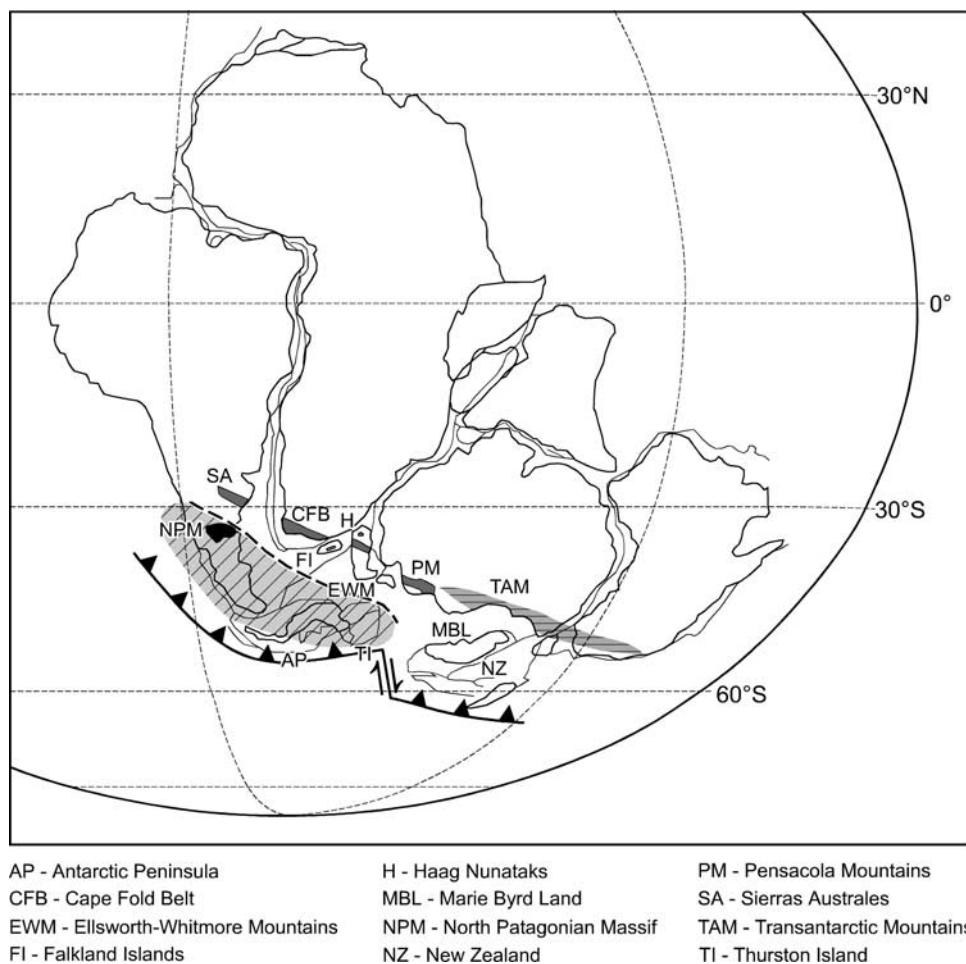


**Figure 21.** Patagonian forearc/arc terrane (diagonally ruled gray area) with North Patagonian Massif (black) in the Gondwanaland reconstruction at the time of the Gondwanide orogeny (modified from the *Dalziel and Grunow* [1992] interpretation which is based on the reconstruction of *Lawver et al.* [1991]). The dashed line indicates the terrane suture.

formation and thrusting within the North Patagonian Massif.

[98] Within the fold-and-thrust belt of the Sierras Australes in the Buenos Aires Province to the north, NE-SW compression led to NE vergent folding combined with the formation of reverse and thrust faults [e.g., *von Gosen et al.*, 1990, 1991]. The latter are directed toward the Claramecó foreland basin in the northeast. The formation of the sigmoidally curved mountain chain has been related either to sinistral transpressive deformation [*Sellés Martínez*, 1986, 1989; cf. *von Gosen et al.*, 1990] or right-lateral transpressive motions [*Cobbold et al.*, 1986, 1991; *Rossello et al.*, 1997]. Isotopic dating and paleomagnetic studies have shown that the Gondwanide deformation was Permian in age [cf., e.g., *Buggisch*, 1987; *von Gosen et al.*, 1990; *Tomezzoli and Vilas*, 1999; *Tomezzoli*, 2001].

[99] The above indicators of a Late Paleozoic deformation across the boundary of Patagonia and to the north show that a common approximately NE-SW compression has affected these areas to a variable extent [see also *Giacosa*, 2001] (present Figure 20). Such a configuration, combined

with the formation of mylonites in different areas, points at an approximately NE-SW collision between Patagonia and South America. The northern margin of extra-Andean Patagonia then can represent a plate boundary also indicated by the inferred margin of the Early Paleozoic Cuyania (Precordillera) Terrane. Collision of Patagonia during Late Paleozoic times might have followed the docking of this terrane. The position of the North Patagonian Massif just aside of the Gondwanide fold belt ("Samfrau Orogenic Zone" of *Du Toit* [1937]) supports the interpretation of a collision during the Gondwanide orogeny (Figure 21).

[100] It should be stated, however, that no ophiolites and/or ocean floor sediments could have been detected in the area north of Patagonia which is widely covered by young sediments. The magmatics in northern Patagonia can be related to subduction along either the Pacific margin in the west [e.g., *Davidson et al.*, 1987; *Uliana and Biddle*, 1987; *Hervé*, 1988; *Cingolani et al.*, 1991] or the northern margin of Patagonia [*Ramos*, 1984, 1986]. The first possibility implies an autochthonous position of Patagonia with an arc plutonism far to the east of the trench and related to a

flat slab subduction. This is supported by results of paleomagnetic studies of *Rapalini* [1998] which indicate that Patagonia did not undergo important latitudinal displacements relative to South America since the Devonian. In such a model of autochthoneity, the Gondwanide deformation can be explained by intraplate compression as proposed by, e.g., *Dalla Salda et al.* [1990] and *Rossello et al.* [1997]. The formation of a compressional back arc basin, related to a wide Andean-type active margin, has been seen as a possible cause for the Gondwanide orogeny by *Trouw and De Wit* [1999].

[101] The long distance between the calc-alkaline plutonism in northeastern Patagonia and the trench in the west as well as the orogenic activity oblique to the Andean trend, however, are arguments against the above interpretation and in favor of subduction along the northern Patagonia margin [Ramos, 1986]. During the Permian, sedimentation in the Sierras Australes, South African Cape Fold Belt, and Ellsworth Mountains of Antarctica records a change from initial craton-derived detritus to arc/orogen-derived material (associated with the deposition of tuffs) and by that indicates the change to developing foreland basins [e.g., *Collinson*, 1991; *López Gamundi et al.*, 1995; *López Gamundi and Rossello*, 1998]. According to *López Gamundi and Rossello* [1998] this suggests that the Sierras Australes and Cape Fold Belt were bordered to the south by an active plate margin.

[102] The long extent of the Gondwanide fold belt from the Sierras Australes to the Cape Fold Belt [e.g., *Keidel*, 1916; *Keidel*, 1939] and Falkland (Malvinas) Islands, with a further continuation in the Ellsworth Mountains and Pensacola Mountains of Antarctica, is inconsistent with an only local intraplate compression zone. It supports the interpretation that Patagonia and related crustal parts on the Pacific side of Gondwana were active as one plate that controlled Gondwanide compression. Hence, a subduction with final collision in the Patagonia and Cape Fold Belt segments [Ramos, 1984, 1986; *De La R. Winter*, 1984; *Johnson*, 1990] cannot be excluded.

[103] In the Gondwanaland reconstruction of *Dalziel and Grunow* [1992], Patagonia has been interpreted as part of a forearc/arc terrane on the Pacific side of Gondwana (Figure 21). According to their interpretation, the Gondwanide orogeny may have been caused by arc-continent collision. They refer collision to the closure of a marginal basin mainly floored by stretched continental crust. This could imply that the Patagonia plate was a detached fragment of the SW Gondwana margin. It can explain the deposition of the Sierra Grande formation and equivalents north of Patagonia and subsequent collisional features in Patagonia and across its northern boundary during the Gondwanide orogeny. It remains unclear, however, whether Patagonia originated and drifted as a terrane from a far-away position, as proposed by *Keppie and Ramos* [1999, Figures 7–9].

## 7. Conclusions

[104] A comparable deformational history in two areas of the northeastern sector of the North Patagonian Massif can be separated into three stages as follows:

1. N-S to NE-SW compression led to S to SW directed thrust tectonics which affected a Late Proterozoic to Cambrian phyllite succession as well as the Silurian to Lower Devonian Sierra Grande formation. Thrusting was combined with the formation of mylonites recording an approximately SW directed sense of shear. They are attributed to a ductile shear horizon in the subsurface. Based on the geometries, a wide extent of folding and thrusting in this part of the North Patagonian Massif is probable. Thrust tectonics was followed by the intrusion of the Navarrete granodiorite and probably is Late Paleozoic in age (? Permian).

2. The formation of widely distributed fold structures around ~NE-SW trending axes and approximately SE directed reverse faults were the effects of ~NW-SE compression. The tectonically stacked thrust sheets were overprinted by these structures. Shortening was accommodated by the formation of a décollement in the subsurface. The uplift of ductilely deformed granitoids took place along an associated reverse fault. During the late stage of deformation, a porphyric granite intruded as final pulse of the Navarrete Intrusive Complex.

3. Local folding around approximately N-S to NW-SE trending axes was the result of an approximately W-E compression and represents the final stage of the deformational history. It was followed by the extrusion of Triassic and Jurassic volcanics accompanied by the intrusion of the Jurassic Flores granite.

[105] Late Paleozoic (probably Permian) thrust tectonics plus subsequent stages of deformation can be seen in conjunction with the formation of granite mylonites in the area west of Mina Gonzalito and in the Cerro de los Viejos of the La Pampa Province, north of the boundary of Patagonia. Furthermore, it can be related to the compressive structures in the Sierras Australes fold-and-thrust belt north of Patagonia.

[106] Taken together, this shows a comparable compression in northern Patagonia and Gondwana South America during the Late Paleozoic, probably the Permian. In this part of the North Patagonian Massif, the lack of clear Early Paleozoic (Famatinian) structures and the inferred boundary of the Early Paleozoic Cuyania (Precordillera) Terrane north of Patagonia (Figure 1) also support the interpretation that extra-Andean Patagonia collided with Gondwana South America during the Gondwanide orogeny. It is possible that Patagonia was part of a plate whose collision zone is represented by the long Gondwanide fold belt.

[107] **Acknowledgments.** I am grateful to E. Llambías, A. Sato, P. González (La Plata), and C. Prozzi (Bahía Blanca) for all the help, discussions, and support during fieldwork in Argentina. Many thanks to J. Ranalli (La Plata) for field assistance and the engagement in solving geological and logistic problems. Discussions with V. Ramos (Buenos Aires), C. Cingolani, L. Spalletti, and R. Varela (La Plata), and the support of E. Bouhier (Dirección de Minas, San Antonio Oeste/Río Negro), are gratefully acknowledged. I am grateful to V. Ramos and R. Pankhurst for constructive reviews which helped to improve the manuscript. The studies were enabled by grants from the German Research Foundation (DFG; Proj. GO 405/4-1 and 4-2). For fieldwork, a car was provided by the Centro de Investigaciones Geológicas (CIG, La Plata). Many thanks to both institutions for their support. This paper is a contribution to IGCP 436.

## References

- Amos, A. J., Silurian of Argentina, in *Correlation of the South American Silurian Rocks*, edited by W. B. N. Berry and A. J. Boucot, *Spec. Pap. Geol. Soc. Am.*, 133, 5–19, 1972.
- Braitsch, O., Das Paläozoikum von Sierra Grande (Prov. Río Negro, Argentinien) und die altkaledonische Faltung im östlichen Andenvorland, *Geol. Rundsch.*, 54, 698–714, 1965.
- Buggisch, W., Stratigraphy and very low grade metamorphism of the Sierras Australes de la Provincia de Buenos Aires (Argentina) and implications in Gondwana correlation, *Zbl. Geol. Paläontol. Teil I*, 7/8, 819–837, 1987.
- Caminos, R., *Geología y Recursos Minerales de la Hoja 4166-I, Valcheta*, 132 pp., Serv. Geol. Min. Argent., Viedma, 1999.
- Caminos, R., and P. Espejo, Hoja Geológica Valcheta 4166-I(1:250,000), Serv. Geol. Min. Argent., Viedma, 1999.
- Caminos, R., and E. J. Llambías, El basamento cristalino, IX Congr. Geol. Argent. Relatorio (Geol. Recur. Nat. Prov. Río Negro), 1(2), 37–63, 1984.
- Caminos, R., E. J. Llambías, C. W. Rapela, and C. A. Parica, Late Paleozoic-Early Triassic magmatic activity of Argentina and the significance of new Rb-Sr ages from northern Patagonia, *J. S. Am. Earth Sci.*, 1, 137–145, 1988.
- Caminos, R., C. Chernicoff, and R. Varela, Evolucion tectónico-metamórfica y edad del Complejo Yaminué, Basamento pre-andino norpatagónico, República Argentina, 7. Congr. Geol. Chil. Actas, II, 1301–1305, 1994.
- Castellaro, H. A., *Guía Paleontológica Argentina, Parte I, Paleozoico, Sección III—Faunas Silúricas, Sección IV—Faunas Devónicas*, pp. 1–164, Cons. Nac. de Invest. Cient. y Tec., Buenos Aires, 1966.
- Chernicoff, C. J., and R. Caminos, Estructura y metamorfismo del Complejo Yaminué, Macizo Nordpatagónico oriental, Provincia de Río Negro, *Rev. Asoc. Geol. Argent.*, 51, 107–118, 1996a.
- Chernicoff, C. J., and R. Caminos, Estructura y relaciones estratigráficas de la Formación Nahuel Niyeu, Macizo Nordpatagónico oriental, Provincia de Río Negro, *Rev. Asoc. Geol. Argent.*, 51, 201–212, 1996b.
- Cingolani, C. A., and R. Varela, The San Rafael Block, Mendoza (Argentina): Rb-Sr isotopic age of the basement rocks, II. Latin Am. Symp. Isotope Geol. (Villa Carlos Paz/Córdoba) Actas, 23–26, 1999.
- Cingolani, C., L. Dalla Salda, F. Hervé, F. Munizaga, R. J. Pankhurst, M. A. Parada, and C. W. Rapela, The magmatic evolution of northern Patagonia: New impressions of pre-Andean and Andean tectonics, in *Andean Magmatism and Its Tectonic Setting*, edited by R. S. Harmon and C. W. Rapela, *Spec. Pap. Geol. Soc. Am.*, 265, 29–44, 1991.
- Cobbold, P. R., A. C. Massabie, and E. A. Rossello, Hercynian wrenching and thrusting in the Sierras Australes foldbelt, Argentina, *Hercynia*, II(2), 135–148, 1986.
- Cobbold, P. R., D. Gapais, and E. A. Rossello, Partitioning of transpressive motions within a sigmoidal foldbelt: The Variscan Sierras Australes, Argentina, *J. Struct. Geol.*, 13(7), 743–758, 1991.
- Collinson, J. W., The palaeo-Pacific margin as seen from East Antarctica, in *Geological Evolution of Antarctica*, edited by M. R. A. Thomson, J. A. Crame, and J. W. Thomson, pp. 199–204, Cambridge Univ. Press, New York, 1991.
- Cortés, J. M., R. Caminos, and H. A. Leanza, La cubierta sedimentaria eopaleozoica, IX Congr. Geol. Argent. Relatorio (Geol. Recur. Nat. Prov. Río Negro), 1(3), 65–84, 1984.
- Criado Roque, P., and G. Ibáñez, Provincia geológica sanrafaelino-pampeana, in *Segundo Simposio de Geología Regional Argentina, 8-II de Septiembre de 1976*, vol. 1, pp. 837–869, Acad. Nac. de Ciencias, Córdoba, Argentina, 1979.
- Dalla Salda, L., C. Cingolani, and R. Varela, The origin of Patagonia, *Rev. Comunic.*, 41, 55–64, 1990.
- Dalla Salda, L. H., C. Cingolani, and R. Varela, Early Paleozoic orogenic belt of the Andes in southwestern South America: Result of Laurentia-Gondwana collision?, *Geology*, 20, 617–620, 1992a.
- Dalla Salda, L. H., I. W. D. Dalziel, C. A. Cingolani, and R. Varela, Did Taconic Appalachians continue into southern South America?, *Geology*, 20, 1059–1062, 1992b.
- Dalla Salda, L., C. Cingolani, and R. Varela, A pre-Carboniferous tectonic model in the evolution of southern South America, *Comptes Rendus 12 Int. Congr. Carboniferous-Permian (Buenos Aires)*, 1, 371–384, 1993.
- Dalla Salda, L. H., R. Varela, C. Cingolani, and E. Aragón, The Río Chico Paleozoic Crystalline Complex and the evolution of Northern Patagonia, *J. S. Am. Earth Sci.*, 7, 377–386, 1994.
- Dalziel, I. W. D., and A. M. Grunow, Late Gondwanide tectonic rotations within Gondwanland, *Tectonics*, 11(3), 603–606, 1992.
- Davidson, J., C. Mpodozis, E. Godoy, F. Hervé, R. Pankhurst, and M. Brook, Late Paleozoic accretionary complexes on the Gondwana margin of southern Chile: Evidence from the Chonos Archipelago, in *Gondwana Six: Structure, Tectonics, and Geophysics*, *Geophys. Monogr. Ser.*, vol. 40, edited by G. D. McKenzie, pp. 221–227, AGU, Washington, D.C., 1987.
- De La R. Winter, H., Tectonostratigraphy, as applied to analysis of South African Phanerozoic basins, *Trans. Geol. Soc. S. Afr.*, 87, 169–179, 1984.
- Du Toit, A. L., *Our Wandering Continents*, 366 pp., Oliver and Boyd, Edinburgh, 1937.
- Fryklund, B., A. Marshall, and J. Stevens, Cuenca del Colorado, in *Geología y Recursos Naturales de la Plataforma Continental Argentina, XIII. Congreso Geológico Argentino y III. Congreso de Exploración de Hidrocarburos, Relatorio*, 8, edited by V. A. Ramos and M. A. Turic, pp. 135–158, Asoc. Geol. Argent., Buenos Aires, 1996.
- Giacosa, R. E., Caracterización de un sector del basamento metamórfico-migmatítico en el extremo suroriental del Macizo Nordpatagónico, Provincia de Río Negro, Argentina, 10. Congr. Geol. Argent. Actas, III, 51–54, 1987.
- Giacosa, R. E., El basamento Precámbrico del sector oriental del Macizo Nordpatagónico, Argentina, *Zbl. Geol. Paläontol., Teil 1*, 1993, 1/2, 89–100, 1994.
- Giacosa, R. E., Zonas de cizalla fragil-ductil en el sector oriental del Macizo Nordpatagónico, XIII. Congr. Geol. Argent. III. Congr. Explor. Hidrocarb. Actas, II, 395, 1996.
- Giacosa, R. E., Geología y petrología de las rocas precretácicas de la región de Sierra Pailemán, Provincia de Río Negro, *Rev. Asoc. Geol. Argent.*, 52, 65–80, 1997.
- Giacosa, R. E., El basamento pre-silúrico del extremo Este del Macizo Nordpatagónico y del Macizo del Deseado, in *Geología Argentina*, edited by R. Caminos, *Inst. Geol. Recur. Miner. Anales*, 29(5), 118–123, 1999.
- Giacosa, R. E., Zonas de cizalla frágil-ductil neopaleozoicas en el nordeste de la Patagonia, *Rev. Asoc. Geol. Argent.*, 56, 131–140, 2001.
- Hervé, F., Late Paleozoic subduction and accretion in southern Chile, *Episodes*, 11(3), 183–188, 1988.
- Hoepfner, R., Tektonik im Schiefergebirge, *Geol. Rundsch.*, 44, 26–58, 1955.
- Huber-Grünberg, A., Sedimentologie, Fazies und Herkunft der kambrisch/ordovizischen und silurisch/unterdevonischen Einheiten von Sierra Grande, Patagonien, dissertation, 196 pp., Univ. of Munich, 1990.
- Johnson, M. R., Provenance and tectonic setting of the Cape-Karoo Basin in the eastern Cape Province, 23rd Earth Sci. Congr. Geol. Soc. S. Afr. (Cape Town) Abstr. Geocongr., 90, 690–693, 1990.
- Kay, S. M., V. A. Ramos, C. Mpodozis, and P. Sruoga, Late Paleozoic to Jurassic silicic magmatism at the Gondwana margin: Analogy to the Middle Proterozoic in North America?, *Geology*, 17, 324–328, 1989.
- Keidel, H., Über die “Gondwaniden” Argentinien, *Geol. Rundsch.*, 30, 148–249, 1939.
- Keidel, J., La geología de las Sierras de la Provincia de Buenos Aires y sus relaciones con las montañas del Cabo y los Andes, *Minist. Agricult. Nac. Direc. Nac. Geol. Miner. Anales*, 9(3), 5–77, 1916.
- Keppie, J. D., and V. A. Ramos, Odyssey of terranes in the Iapetus and Rheic oceans during the Paleozoic, in *Laurentia-Gondwana Connections Before Pangea*, edited by V. A. Ramos and J. D. Keppie, *Spec. Pap. Geol. Soc. Am.*, 336, 267–276, 1999.
- Lawver, L. A., J.-Y. Royer, D. T. Sandwell, and C. R. Scotese, Evolution of the Antarctic continental margins, in *Geological Evolution of Antarctica*, edited by M. R. A. Thomson, J. A. Crame, and J. W. Thomson, pp. 533–539, Cambridge Univ. Press, New York, 1991.
- Limarino, C. O., A. Massabie, E. Rossello, O. López Gamundi, R. Page, and G. Jalfin, El Paleozoico de Ventania, Patagonia e Islas Malvinas, in *Geología Argentina*, edited by R. Caminos, *Inst. Geol. Recur. Miner. Anales*, 29(13), 319–347, 1999.
- Linares, E., E. J. Llambías, and C. O. Latorre, Geología de la Provincia de La Pampa, República Argentina y geocronología de sus rocas metamórficas y eruptivas, *Rev. Asoc. Geol. Argent.*, 35, 87–146, 1980.
- Linares, E., H. A. Ostera, and C. A. Parica, Edades radiométricas preliminares del basamento cristalino de las vicinidades de Mina Gonzalito y de Valcheta, Provincia de Río Negro, República Argentina, 11. Congr. Geol. Argent. Actas, II, 251–253, 1990.
- Llambías, E. J., El magmatismo gondwánico durante el Paleozoico superior-Triásico, in *Geología Argentina*, edited by R. Caminos, *Inst. Geol. Recur. Miner. Anales*, 29(14), 349–363, 1999.
- Llambías, E. J., R. N. Melchor, H. Tickyj, and A. M. Sato, Geología del bloque del Chadileuvú, XIII. Congr. Geol. Argent. III. Congr. Explor. Hidrocarb. Actas, I, 417–425, 1996.
- López Gamundi, O. R., and E. A. Rossello, Basin fill evolution and paleotectonic patterns along the Samfrau geosyncline: the Sauce Grande basin-Ventana foldbelt (Argentina) and Karoo basin-Cape foldbelt (South Africa) revisited, *Geol. Rundsch.*, 86, 819–834, 1998.
- López-Gamundi, O. R., P. J. Conaghan, E. A. Rossello, and P. R. Cobbold, The Tunas Formation (Permian) in the Sierras Australes Foldbelt, east central Argentina: Evidence for syntectonic sedimentation in a foreland basin, *J. S. Am. Earth Sci.*, 8, 129–142, 1995.
- Melchor, R. N., A. M. Sato, E. J. Llambías, and H. Tickyj, Documentación de la extensión meridional del terreno Cuyania/Precordillera en la provincia de La Pampa, XIV. Congr. Geol. Argent. Actas, I, 156–159, 1999.
- Müller, H., Zur Altersfrage der Eisenerzlagerstätte Sierra Grande/Río Negro in Nordpatagonien aufgrund neuer Fossilfunde, *Geol. Rundsch.*, 54, 715–732, 1965.
- Pankhurst, R. J., C. W. Rapela, R. Caminos, E. Llambías, and C. Parica, A revised age for the granites of the central Somuncura Batholith, North Patagonian Massif, *J. S. Am. Earth Sci.*, 5(3/4), 321–325, 1992.
- Pankhurst, R. J., R. Caminos, and C. W. Rapela, Problemas geocronológicas de los granitoides gondwánicos de Nahuel Niyeu, Macizo Nordpatagónico, XII. Congr. Geol. Argent. II. Congr. Explor. Hidrocarb. Actas, II, 99–104, 1993.
- Pankhurst, R. J., C. W. Rapela, and C. M. Fanning, The Mina Gonzalito Gneiss: Early Ordovician meta-

- morphism in northern Patagonia, III. S. Am. Symp. Isotope Geol. (Santiago Soc. Geol. Chile) Extended Abstr. (CD), 604–207, 2001.
- Ramos, V. A., Geología del sector oriental del Macizo Nordpatagónico entre Aguada Capitan y la Mina Gonzalito, Provincia de Río Negro, *Rev. Asoc. Geol. Argent.*, 30, 274–285, 1975.
- Ramos, V. A., Patagonia: ¿Un continente Paleozoico a la deriva?, IX. Congr. Geol. Argent. Actas, II, 311–325, 1984.
- Ramos, V. A., Tectonostratigraphy, as applied to analysis of South African Phanerozoic basins by H. De La R. Winter-Discussion, *Trans. Geol. Soc. S. Afr.*, 89, 427–429, 1986.
- Ramos, V. A., Late Proterozoic-Early Paleozoic of South America—A collisional history, *Episodes*, 11(3), 168–174, 1988.
- Ramos, V. A., Evolución tectónica de la plataforma continental, in *Geología y Recursos Naturales de la Plataforma Continental Argentina*, XIII. Congr. Geol. Argent. y III. Congr. Explor. Hidrocarb., *Relatorio*, 21, edited by V. A. Ramos and M. A. Turic, pp. 385–404, Asoc. Geol. Argent., 1996.
- Rapalini, A., La edad de la tectónica en la Formación Sierra Grande, en base a estudios de remanencia y fabrica magnéticas, XIII. Congr. Geol. Argent. III. Congr. Explor. Hidrocarb. Actas, 2, 475, 1996.
- Rapalini, A. E., Syntectonic magnetization of the mid-Palaeozoic Sierra Grande Formation: Further constraints on the tectonic evolution of Patagonia, *J. Geol. Soc. London*, 155, 105–114, 1998.
- Rapela, C. W., and S. M. Kay, Late Paleozoic to recent magmatic evolution of northern Patagonia, *Episodes*, 11(3), 175–182, 1988.
- Rossello, E. A., A. C. Massabie, O. R. López-Gamundi, P. R. Cobbold, and D. Gapais, Late Paleozoic transpression in Buenos Aires and northeast Patagonia ranges, Argentina, *J. S. Am. Earth Sci.*, 10, 389–402, 1997.
- Rossi, E. E., and J. C. M. Zanettini, Prospección geológico-geofísica de mineral de hierro en las provincias de Río Negro y Chubut, *Rev. Asoc. Geol. Argent.*, 41, 233–244, 1986.
- Sato, A. M., H. Tickyj, E. J. Llambías, and K. Sato, Rb-Sr, Sm-Nd and K-Ar age constraints of the Grenvillian Las Matras pluton, Central Argentina, II. Latin Am. Symp. Isotope Geol. (Villa Carlos Paz/Córdoba) Actas, 122–126, 1999.
- Sato, A. M., H. Tickyj, E. J. Llambías, and K. Sato, The Las Matras tonalitic-trondhjemitic pluton, central Argentina: Grenvillian-age constraints, geochemical characteristics, and regional implications, *J. S. Am. Earth Sci.*, 13, 587–610, 2000.
- Sellés Martínez, J., Las Sierras Australes de Buenos Aires: Su vinculación a un cizallamiento regional, *Rev. Asoc. Geol. Argent.*, 41, 187–190, 1986.
- Sellés Martínez, J., The structure of the Sierras Australes (Buenos Aires Province, Argentina): An example of folding in a transpressive environment, *J. S. Am. Earth Sci.*, 2, 317–329, 1989.
- Stipanovic, P. N., and E. J. Methol, Comarca Norpatagónica, in *Segundo Simposio de Geología Regional Argentina*, 8-11 de Septiembre de 1976, vol. 2, pp. 1071–1097, Acad. Nac. de Ciencias, Córdoba, Argentina, 1980.
- Tickyj, H., and E. Llambías, El gneis milonítico del Cerro de los Viejos (38°28'S–64°26'O), Provincia de La Pampa, Argentina. ¿Evidencia de un corrimiento en el Carbonífero inferior?, 7. Congr. Geol. Chileno Actas, II, 1239–1243, 1994.
- Tickyj, H., L. V. Dimieri, E. J. Llambías, and A. M. Sato, Cerro de Los Viejos (38°28'S–64°26'O): Cizallamiento dúctil en el sudeste de La Pampa, *Rev. Asoc. Geol. Argent.*, 52, 311–321, 1997.
- Tickyj, H., E. J. Llambías, and A. M. Sato, El basamento cristalino de la región sur-oriental de la Provincia de La Pampa: Extensión austral del Orogénico Famatiniano de Sierras Pampeanas, XIV. Congr. Geol. Argent. Actas, I, 160–163, 1999a.
- Tickyj, H., M. A. Stipp Basei, A. M. Sato, and E. J. Llambías, U-Pb and K-Ar ages of Pichi Mahuida Group, crystalline basement of south-eastern La Pampa Province, Argentina, II. Latin Am. Symp. Isotope Geol. (Villa Carlos Paz/Córdoba) Actas, 139–142, 1999b.
- Tomezzoli, R. N., Further palaeomagnetic results from the Sierras Australes fold and thrust belt, Argentina, *Geophys. J. Int.*, 147, 356–366, 2001.
- Tomezzoli, R. N., and J. F. Vilas, Palaeomagnetic constraints on the age of deformation of the Sierras Australes thrust and fold belt, Argentina, *Geophys. J. Int.*, 138, 857–870, 1999.
- Trouw, R. A. J., and M. J. De Wit, Relation between the Gondwanide Orogen and contemporaneous intracratonic deformation, *J. Afr. Earth Sci.*, 28, 203–213, 1999.
- Uliana, M. A., and K. T. Biddle, Permian to Late Cenozoic evolution of northern Patagonia: main tectonic events, magmatic activity, and depositional trends, in *Gondwana Six: Structure, Tectonics, and Geophysics*, *Geophys. Monogr. Ser.*, vol. 40, edited by G. D. McKenzie, pp. 271–286, AGU, Washington, D.C., 1987.
- Varela, R., C. Cingolani, A. Sato, L. Dalla Salda, B. B. Brito Neves, M. A. S. Basei, O. Siga Jr., and W. Teixeira, Proterozoic and Paleozoic evolution of Atlantic area of North-Patagonian Massif, Argentine, S. Am. Symp. Isotope Geol. (Sao Paulo/Brazil, June 15–18, 1997) Extended Abstr., 326–329, 1997.
- Varela, R., M. A. S. Basei, A. M. Sato, O. Siga Jr., C. A. Cingolani, and K. Sato, Edades isotópicas Rb/Sr y U/Pb en rocas de Mina Gonzalito y Arroyo Salado. Macizo Norpatagónico Atlántico, Río Negro, Argentina, X. Congr. Latinoam. Geol. VI. Congr. Nac. Geol. Econ. Actas, I, 71–76, 1998.
- von Gosen, W., Polyphase structural evolution in the northeastern segment of the North Patagonian Massif (southern Argentina), *J. S. Am. Earth Sci.*, in press, 2002.
- von Gosen, W., and W. Buggisch, Entwicklung und Bau der Sierras Australes (Provinz Buenos Aires, Argentinien), *Erlanger Geol. Abh.*, 116, 21–34, 1988.
- von Gosen, W., and C. Prozzi, Structural evolution of the Sierra de San Luis (Eastern Sierras Pampeanas, Argentina: Implications for the Proto-Andean Margin of Gondwana, in *The Proto-Andean Margin of Gondwana*, edited by R. J. Pankhurst and C. W. Rapela, *Geol. Soc. Spec. Publ.*, 142, 235–258, 1998.
- von Gosen, W., W. Buggisch, and L. V. Dimieri, Structural and metamorphic evolution of the Sierras Australes (Buenos Aires Province/Argentina), *Geol. Rundsch.*, 79, 797–821, 1990.
- von Gosen, W., W. Buggisch, and S. Krumm, Metamorphism and deformation mechanisms in the Sierras Australes fold and thrust belt (Buenos Aires Province, Argentina), *Tectonophysics*, 185, 335–356, 1991.

---

W. von Gosen, Geological Institute, University of Erlangen-Nürnberg, Schlossgarten 5, D-91054 Erlangen, Germany. (vgosen@geol.uni-erlangen.de)